scientific reports



OPEN Comparative proteomic profiling of the ovine and human PBMC inflammatory response

A. Elkhamary^{1,2,5}, I. Gerner^{1,3,5}, A. Bileck⁴, G. L. Oreff¹, C. Gerner^{4,6} & F. Jenner^{1,3,6⊠}

Understanding the cellular and molecular mechanisms of inflammation requires robust animal models. Sheep are commonly used in immune-related studies, yet the validity of sheep as animal models for immune and inflammatory diseases remains to be established. This cross-species comparative study analyzed the in vitro inflammatory response of ovine (oPBMCs) and human PBMCs (hPBMCs) using mass spectrometry, profiling the proteome of the secretome and whole cell lysate. Of the entire cell lysate proteome (oPBMCs: 4217, hPBMCs: 4574 proteins) 47.8% and in the secretome proteome (oPBMCs: 1913, hPBMCs: 1375 proteins) 32.8% were orthologous between species, among them 32 orthologous CD antigens, indicating the presence of six immune cell subsets. Following inflammatory stimulation, 71 proteins in oPBMCs and 176 in hPBMCs showed differential abundance, with only 7 overlapping. Network and Gene Ontology analyses identified 16 shared inflammatory-related terms and 17 canonical pathways with similar activation/inhibition patterns in both species, demonstrating significant conservation in specific immune and inflammatory responses. However, ovine PMBCs also contained a unique WC1*γδT-cell subset, not detected in hPBMCs. Furthermore, differences in the activation/inhibition trends of seven canonical pathways and the sets of DAPs between sheep and humans, emphasize the need to consider interspecies differences in translational studies and inflammation research.

Inflammation is a double-edged sword in maintaining health and disease, integral to both the physiologic response to injury or infection and, when chronic, the pathogenesis of most chronic diseases, including cardiovascular disease, diabetes, osteoarthritis and cancer in both humans and animals¹⁻⁹. Indeed, chronic inflammatory diseases globally account for more than 50% of all deaths, making them the most significant cause of morbidity and mortality^{2,3}.

Inflammation is an evolutionarily conserved protective response to external and internal injurious stimuli, such as invading pathogens, toxins or damaged cells. It serves to eliminate the noxae, clear necrotic cells, initiate tissue repair and restore tissue homeostasis^{4,6–15}. The inflammatory response starts when tissuE-resident sentinel cells' pattern recognition receptors detect pathogen- or damage-associated molecular patterns. This triggers the secretion of inflammatory cytokines, leading to the recruitment of neutrophils and peripheral blood mononuclear cells (PBMCs) for phagocytosis and elimination of tissue debris and microorganisms^{4,6-15}. Recruited leukocytes, activated by the local inflammatory environment, adopt an inflammatory phenotype, secreting proteases, chemokines, and cytokines, amplifying inflammation 16-18. However, acute inflammation is typically short-lived and subsides once the trigger is eliminated 18-34. Thereafter, macrophages clear apoptotic neutrophils through efferocytosis, initiating their functional repolarization to a pro-resolving phenotype and biosynthesis of proresolving mediators that promote the return to homeostasis 18-34. Thus, the delicate balance between an effective defensive response, collateral tissue damage and persistent inflammation hinges on the tightly coordinated regulation of pro-inflammatory and pro-resolving cytokine secretion¹⁸⁻³⁴. However, the intricate signaling cascades orchestrating an inflammatory response and its resolution or transition to chronic inflammation remain to be fully elucidated.

Moreover, during both systemic inflammatory responses and localized inflammatory reactions, cytokines, such as interleukin (IL)-6 and tumor necrosis factor (TNF)-α, are released into the bloodstream, orchestrating

¹Department for Companion Animals and Horses, Veterm, University Equine Hospital, Vetmeduni Vienna, Vienna, Austria. ²Department for Surgery, Faculty of Veterinary Medicine, Damanhour University, Damanhour, Egypt. ³Austrian Cluster for Tissue Regeneration, Vienna, Austria. ⁴Department of Analytical Chemistry, Faculty of Chemistry, University of Vienna, Vienna, Austria. 5These authors contributed equally: A. Elkhamary and I. Gerner. ⁶These authors jointly supervised this work: C. Gerner and F. Jenner. [∞]email: florien.jenner. ⓐ vetmeduni.ac.at

a range of circulating immune cell activities, including activation, differentiation, and recruitment, while also triggering systemic responses, such as the stimulation of liver hepatocytes to synthesize and release acute phase proteins^{35–37}. Consequently, the levels of peripheral blood cytokines have emerged as a crucial diagnostic and prognostic biomarker for both systemic and localized inflammatory responses, offering potential applications in the assessment of therapeutic efficacy and the optimization of treatment strategies in various diseases, including sepsis, asthma, atherosclerosis and osteoarthritis³⁸⁻⁴⁰. Given that direct measurement of cytokines in affected tissues often necessitate tissue biopsy and cytokine detection in serum or plasma is challenging due to the short half-lives of many cytokines, their binding to soluble receptors or carrier proteins and the analytical difficulties originating from highly abundant plasma proteins, the measurement of cytokine production by peripheral blood mononuclear cells (PBMCs) has become a widely adopted approach for assessing inflammatory responses^{41–51}. PBMCs, a readily accessible blood cell fraction comprised predominantly of lymphocytes and monocytes, play a crucial role in in mediating both innate and adaptive immune responses, regulating inflammation and maintaining immune homeostasis 41-52. They act as sentinel cells, providing a real-time reflection of the cellular and humoral immune status state of the entire body^{46,53–55}. Notably, the proteome of PBMCs has been demonstrated to correlate with the presence and progression of various diseases, including chronic obstructive pulmonary disease, rheumatoid arthritis, leukemia, pancreatic cancer, metabolic syndrome and sepsis^{41–52,56}. Therefore, PBMCs are extensively employed as ex vivo cellular model in immunological studies to investigate immune responses across diverse inflammatory conditions, analyze diagnostic and prognostic biomarkers, identify potential immunotherapy targets, and assess the efficacy of immunomodulatory therapies^{47,50,57–59}.

While in vitro or ex vivo assays with human immune cells offer valuable insights into immune function, they are unable to fully replicate the complex cellular and molecular interactions involved in immune responses 47,50,57-59. Recognizing this limitation, the One Health initiative emphasizes the importance of companion animals as models for human disease, aiming to bridge the gap between medical and veterinary research for the benefit of both⁶⁰. This necessitates the utilization of animal models for specific indications, with sheep, due to their anatomical and physiological similarities to humans, including organ size and longevity, emerging as widely used biomedical models $^{61-63}$. These similarities encompass various systems, such as the cardiovascular and musculoskeletal system, where sheep and humans share characteristics in valve anatomy, heart rate, blood pressure, aorta size, hemodynamic flow parameters, weight, mechanical properties, joint structure, and bone architecture and remodeling processes⁶⁴⁻⁷². Immunologically, both species exhibit cell-mediated and antibodymediated responses to pathogens and antigens, and possess analogous immune organ structures^{62,66,67}. Sheep respond to LPS challenges at doses comparable to human levels and utilize similar signaling pathways to activate immune responses⁶⁶⁻⁷⁰. Additionally, unlike small rodents, sheep exhibit population diversity through outbreeding and have a well-developed peripheral immune system by the time of birth⁶⁶⁻⁷⁰. Studies in sheep have significantly contributed to our understanding of the ontogeny and organization of the mammalian immune system^{62,63}. However, the definitive establishment of the validity of sheep as animal models for immune and inflammatory diseases remains an ongoing pursuit. To validate sheep as models for the human immune system and inflammatory response, a comprehensive characterization of the cellular composition of sheep PBMCs and their immunological responses is imperative, which to date has been impeded by the limited array of available immunological tools^{63,69,73}. Leveraging the well-documented high functional conservation observed in homologous proteins across species, with human and sheep proteins sharing approximately 93% amino acid identity⁶³, mass spectrometry-based proteomics can facilitate immunophenotyping of PBMCs and characterization of their functional states⁷⁴⁻⁷⁷. A cross-species analytic approach also enables the identification of evolutionarily conserved hub proteins and pathways 78-88, which, in turn, can inform the development of effective therapeutic strategies. Given that drug targets exhibit higher inter-species conservation than other genes and proteins, the co-occurrence of differential regulation in multiple species can be exploited for the identification and prioritization of therapeutic targets^{78–88}.

Therefore, this cross-species comparative proteomics study aims to assess the suitability of the ovine model for replicating human immune signatures and inflammatory pathways by (1) establishing a protocol to isolate ovine PBMCs with cell ratios that closely resemble those found in hPBMCs to ensure accurate and meaningful comparisons in downstream analyses of ovine and human inflammatory responses, (2) identifying cell surface markers for ovine PBMCs using mass spectrometry based on human orthologs to facilitate comparison of PBMC composition and immunophenotype between studies, and (3) comparing the proteomic response of ovine and human PBMCs to inflammation integrating signals not only across orthologous individual molecules (proteins) but also at the level of functional sets, complexes, and pathways, where higher conservation is both expected and functionally more relevant.

Materials and methods Sample collection and ethics approval

This study was carried out using peripheral blood obtained by venipuncture from the jugular vein of six healthy adult, 3–4-year-old Merino ewes, with ethical approval by the institutional ethics and animal welfare committee and the national authority (license BMWF-68.205/0116-V/3b/2018). All methods were performed in accordance with the relevant guidelines and regulations implemented at the University of Veterinary Medicine Vienna, the Institutional Ethics Committee ("Ethics and Animal Welfare Committee") of the University of Veterinary Medicine Vienna.

All sheep included in the study were in a similar reproductive period (nongravid seasonal polyestrous) to ensure consistency in physiological conditions. They were confirmed to be systemically healthy by physical examination and the absence of hematologic abnormalities on complete blood count (CBC). Samples for CBC were subjected to routine blood cytometry performed by the University's certified diagnostic laboratory within

less than 3 h of collection. For oPBMCs isolation, 50 ml of venous whole blood were aseptically collected from the jugular vein into a heparinized (Gilvasan, 5000 IU/ml, 1 ml of Heparin/10 ml of blood) 100-mL syringe through a 23-gauge butterfly catheter. All samples were transferred to the lab and processed immediately after blood collection.

Ovine PBMCs isolation

The protocol for isolating oPBMCs was optimized, considering a diverse array of published technical parameters⁸⁹⁻¹⁰² and accounting for the differences in the physical properties of ovine and human blood ^{103,104}. The optimization process included three primary variables: the dilution of blood samples, the selection of an appropriate density gradient medium, and the precise settings for centrifugation, encompassing both force and duration (Fig. 1a).

To determine the optimal ratio for blood dilution, anti-coagulated whole blood (n = 3 donors) was used either undiluted or diluted in a 1:1 or 1:2 ratio with complete RPMI1640 medium (Gibco, Life Technologies, Austria). This medium was supplemented with 10% heat-inactivated fetal calf serum (Gibco, Life Technologies, Austria), and 1% Penicillin, Streptomycin, and Amphotericin (Sigma-Aldrich, Germany,complete medium). The processed blood samples were then layered over three different density gradient media: Ficoll-Paque PREMIUM* (1.077 g/ml gradient, Cytiva, Sweden), Percoll* (1.130 g/ml gradient, GE Healthcare Bioscience, Sweden), and Lymphoprep* (1.077 g/ml, STEMCELL Technologies, Germany). These samples underwent centrifugation at three different centrifugation forces: 300×g, 660×g, and 800×g, each for a duration of 30 or 60 min (min), at 21 °C, and without brakes. The result of these experiments was ranked according to the quality of separation and perturbation of the different layers (Erythrocyte/Granulocyte layer, density gradient medium, PBMC layer, Plasma layer) (Fig. 1b).

Subsequently, the two density gradient media (Ficoll 1.077 g/ml versus Lymphoprep 1.077 g/ml) and centrifugation times $(660\times g/30 \text{ min versus } 660\times g/60 \text{ min})$, that achieved the best separation quality, were selected for further optimization, aiming to identify the protocol yielding the highest PBMC count with minimal granulocyte contamination. To this end, PBMCs were collected from the medium-plasma interface using a sterile pipet into a 50 ml conical tube and washed once at $540\times g$ for 10 min at 21 °C using 20 ml of PBS without calcium and magnesium (PBS-/-). Then, 5 ml erythrocyte lysis buffer, composed of 154 mM ammonium chloride, 10 mM potassium hydrogencarbonate, and 0.1 mM Ethylenediaminetetraacetic acid), was added to the cell pellet. The tube was gently shaken to facilitate dissolution of the pellet, incubated for 5 min on ice, then mixed with 15 mL of PBS-/-, and centrifuged at $450\times g$ for 5 min at 21 °C. Finally, the supernatant was discarded, and the cell pellet

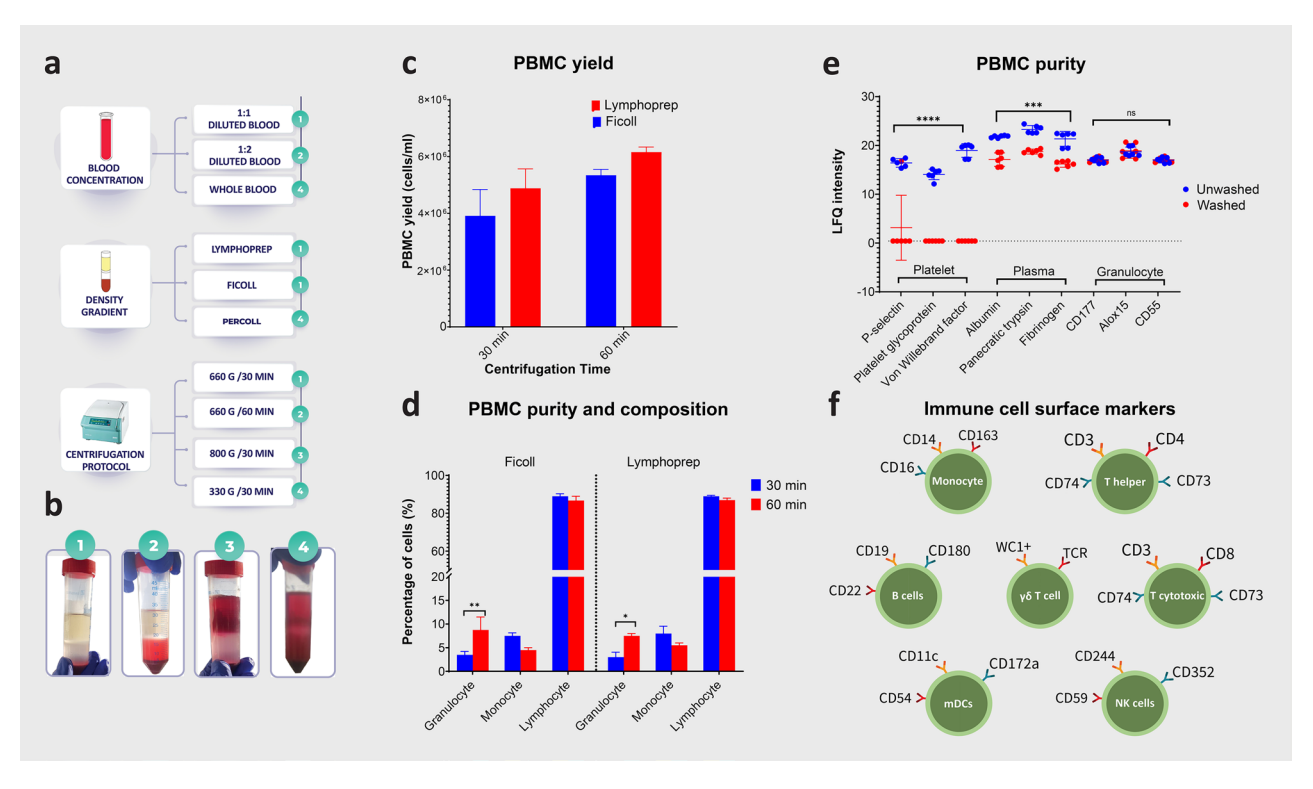


Figure 1. Optimization of the ovine peripheral blood mononuclear cell (oPBMC) isolation protocol. (a) Optimization of the blood dilution, density gradient and centrifugation parameters based on (b) PBMC separation quality. Selection of the density gradient based on (c) PBMC yield and (d) PBMC purity and composition. (e) Mass Spectrometry assessment of purity based on granulocyte-specific cluster of differentiation (CD) antigens and specific proteins associated with platelets and plasma. (f) Mass Spectrometry-based identification of orthologous CD antigens, indicating the presence of seven immune cell subsets.

was washed twice using 10 ml of washing solution (PBS-/- with 2% FCS) and centrifugation at 440×g for 5 min at 21 °C. After the final wash and removal of the supernatant, the PBMCs pellet was processed for further analysis.

The yield of PBMCs was quantified by counting live cells per unit volume, determined by microscopic enumeration using a Neubauer hemocytometer. Cell viability was defined as the proportion of live cells in a population, assessed by their ability to exclude Trypan blue dye. The composition and purity of PBMCs were quantified using the ADVIA 2120i Hematology System™ Automated Cell Counter (Siemens, Germany). The composition of PBMCs was determined by calculating the ratio of isolated lymphocytes and monocytes to the total number of isolated PBMCs population (no monocytes/no PBMCs and no lymphocyte /no PBMCs), with the results expressed as percentage. The purity was determined as the percentage of PBMCs in the total isolated leukocyte population, with a specific emphasis on assessing contamination with other cell types such as granulocytes and erythrocytes. To ensure the suitability of the isolated PBMCs for downstream applications, stringent criteria were set, demanding a minimum viability of 95% and a purity exceeding 95% 105,106.

Proteomic phenotypic characterization of isolated oPBMCs

Due to the limited availability of ovine-specific antibodies essential for immunophenotyping techniques such as flow cytometry analyses ^{63,73}, oPBMCs were phenotypically characterized using MS-based proteomic analyses of lineage specific surface markers. The composition of PBMCs was determined based on the expression of cell type markers, while their purity was determined based on the presence or absence of granulocyte-specific CD antigens and specific proteins associated with platelets and plasma.

The PBMCs pellets were resuspended in serum-free medium (RPMI 1640 medium supplemented with 1% Penicillin, Streptomycin, and Amphotericin (Sigma-Aldrich, Germany) at a concentration of 4×10^6 cells/ml. The cell suspension was plated into a T-25 flask (Greiner Bio-One, Kremsmünster, Austria) at a seeding density of 0.6×10^6 cells per flask and incubated for 3 h at 37 °C in a humidified 5% CO2 incubator.

After the incubation time of the PBMCs, the conditioned medium was harvested into a 15 ml falcon tube, leaving approximately 1 ml medium in the culture flask. The adherent cells remaining in the flask were then gently detached using a cell scraper and combined with the previously transferred conditioned medium in the falcon tube. The cell suspension was centrifuged at $540\times g$ for 5 min at 4 °C to pellet the cells and separate the supernatant. The supernatant was transferred into a new 15 ml falcon tube, centrifuged at $2000\times g$ for 10 min at 4 °C and filtered through a 0.2 μ m filter to remove potential remaining cells and cell debris. The filtered secretome was precipitated on ice cold 99.6% ethanol and stored at – 20 °C until further processing for isolation of secreted proteins.

The cell pellet obtained from the initial centrifugation was washed twice with 5 ml PBS-/- and centrifugation at $540\times g$ for 5 min at 4 °C. Following the removal of the final wash solution, 200 μ l of Sodium deoxycholate lysis bufferer (SDC) (4% sodium deoxycholate, 100 mM Tris HCl pH 8.5) was added to the cell pellet. The mixture was then heated at 95 °C in the water bath for 5 min to ensure complete lysis of the cells. The lysate was subsequently stored at – 80 °C until further proteomic processing for isolation cell lysate proteins.

The secretome and cell lysates obtained from unwashed PBMCs were used as control samples for the evaluation of cell purity. These cells were directly plated after the RBC lysis step as donor-matched control for each PBMC sample, bypassing the final two washing cycles, and were then designated for subsequent culture and analysis via mass spectrometry to measure cell type specific CD markers and specific proteins associated with platelets and plasma.

Inflammatory stimulation oPBMCs

For a standardized assessment of inflammatory responses between ovine and human PBMCs, we adopted an inflammation induction protocol in oPBMCs consistent with the approach used for hPBMCs we previously described ¹⁰⁷.

In brief, isolated oPBMCs (n = 3 biological replicates (3 donors), 3 technical replicates/donor/experimental group) were resuspended to a final concentration of 4×10^6 cells/ml in the complete RPMI 1640 medium supplemented with 1 µg/ml of lipopolysaccharide (LPS, Sigma-Aldrich, Merck, Darmstadt, Germany) in combination with 5 µg/ml of Phytohaemagglutinin (PHA, Sigma-Aldrich). The cell suspension was then seeded into a T-25 flask (Greiner Bio-One, Kremsmünster, Austria) at a density of 0.6×10^6 cells per flask and incubated at 37 °C in 5% CO2 for 6 h. PBMCs cultured in complete RPMI 1640 medium without LPS or PHA served as healthy control samples. Following the 6-h period of inflammatory stimulation, the culture medium was changed to serum-free RPMI medium and further incubated at 37 °C in 5% CO2 for 3 h. Finally, both the secretome and cells were harvested for mass spectrometry analyses, as detailed previously in "Proteomic phenotypic characterization of isolated oPBMCs" section.

Shotgun proteomics by LC-MS/MS

A quantitative LC–MS/MS of both the oPBMCs cell lysate and secretome of the washed versus unwashed PBMCs, as well as stimulated versus untreated PBMCs in sheep, was carried out.

Sample preparation

Proteomic samples were prepared using a modified version of a previously described protocol 108 and employing an adapted version of the EasyPhos platform 109 . PBMC cell pellets were thawed, and further lysed using the S220 Focused-ultrasonicator (Covaris, LLC., Woburn, MA, USA). The precipitated secretome proteins were centrifuged at $5000\times g$ for 30 min at 4 °C and the resulting protein pellet was solubilized in SDC buffer. Protein concentrations were determined via bicinchoninic acid assay (BCA)-assay. Protein (20 µg/sample) was reduced and alkylated with tris(2-carboxyethyl) phosphine (TCEP) and 2-chloroacetamide (2-CAM) for 5 min at 45 °C,

followed by 18 h digestion with Trypsin/Lys-C (1:100 enzyme-to-substrate ratio) at 37 °C, and dried in a vacuum concentrator. Then, the samples were reconstituted in styrenedivinylbenzene-reverse phase sulfonate (SDB-RPS) loading buffer (99% iPrOH, 1% TFA) and desalted via SDB-RPS StageTips. Desalted global proteome samples were reconstituted in 5 μ l formic acid (30%) containing synthetic standard peptides at 10 fmol and diluted with 40 μ l loading solvent (98% H2O, 2% ACN, 0.05% TFA).

LC-MS/MS analysis

LC–MS/MS analyses were performed employing a timsTOF Pro mass spectrometer (Bruker Daltonics, Bremen, Germany) hyphenated with a Dionex UltiMateTM 3000 RSLCnano system (Thermo Scientific, Bremen, Germany). Samples were analyzed in data-dependent acquisition mode by label free quantification (LFQ) shotgun proteomics similarly to a recently published method 108 . The injection volume was 2 μ l for cell lysates and 5 μ l for secretomes, respectively. Samples were loaded on an AcclaimTMPepMapTM C18 HPLC pre-column (2 cm × 100 μ m, 100 Å, Thermo Fisher Scientific. Vienna, Austria) at a flow rate of 10 μ l min-1 MS loading buffer. After trapping, peptides were eluted at a flow rate of 300 nl min-1 and separated on an Aurora series CSI UHPLC emitter column (25 cm × 75 μ m, 1.6 μ m C18, Ionopticks, Fitzroy, Australia) applying a gradient of 8–40% mobile phase B (79.9% ACN, 20% H2O, 0.1% FA) in mobile phase A (99.9% H2O, 0.1% FA) over 85 min.

LC-MS/MS data analyses

Protein identification was performed via MaxQuant¹¹⁰ (version 1.6.17.0) employing the Andromeda search engine against the UniProt Database¹¹¹ (version 11/2021, 20' 375 entries). Search parameters were set as previously described¹⁰⁸. A mass tolerance of 20 ppm for MS spectra and 40 ppm for MS/MS spectra, a PSM-, protein-and site-false discovery rate (FDR) of 0.01 and a maximum of two missed cleavages per peptide were allowed. Match-between-runs were enabled with a matching time window of 0.7 min and an alignment time window of 20 min. Oxidation of methionine and N-terminal protein acetylation were set as variable modifications. Carbamidomethylation of cysteine was set as fixed modification. Proteome data analysis was performed via Perseus (version 1.6.14.0). Proteins with at least 70% quantification rate in at least one group were considered for analysis.

Bioinformatics and statistical analyses

Differentially abundant proteins

To compare the inflammatory responses and pathways between ovine and human PBMCs, proteomics data from oPBMCs were juxtaposed with that of hPBMCs, with both sets inflamed and analyzed through the same methodological approach¹⁰⁷. The mass spectrometry proteomics data of hPBMCs were retrieved from the ProteomeXchange Consortium through the proteomics identification database (PRIDE) repository with the dataset identifier PXD001415 (https://doi.org/10.6019/PXD001415).

A two-sided Student's t test was performed to examine differences between the control group and activated group, and the difference in abundance level between the two groups was calculated. Proteins satisfying a false discovery rate (FDR) \leq 0.05 (used as the threshold of the q-value) and fold change (FC) $\mid \geq 2 \mid$ were considered to be significantly different (differentially abundant proteins, DAPs).

Enrichment analysis

Gene Ontology (GO) and Kyoto Encyclopedia of Genes and Genomes (KEGG) pathway enrichment analyses of the DAPs were performed using the Search Tool for Retrieval of Interacting Genes/proteins (STRING) database (version 11.5, https://string-db.org/)¹¹¹⁻¹¹⁶ with a cut-off p < 0.05. The DAPs were assigned to their corresponding Gene Ontology branches (Biological Process, Molecular Function, and Cellular Component) and KEGG pathways, employing a species-specific background dataset for accurate comparison. Interactions analyzed were strictly confined to those substantiated by experimental evidence.

Protein-protein-interaction network construction and module analysis

Protein–protein interaction (PPI) networks were constructed using STRING (version 11.5; https://string-db.org), applying active interaction sources supported by experiments and an interaction score $\geq 0.4^{117}$, to identify functional interactions of DAPs. The PPI Networks were visualized and analyzed using the Cytoscape software (version 3.9.1, www.cytoscape.org) and its Molecular Complex Detection (MCODE) and CytoHubba plugins $^{118-120}$. MCODE was employed to identify the main clusters in the PPI networks applying a degree cutoff = 2, node score cutoff = 0.2, K-core = 2, max. depth = 100, and haircut cluster finding setting as visualization criteria 119 . Clusters with a score ≥ 5 were considered significant subnetworks. With these clusters as input, we used STRING again to construct the second PPI network for further comprehensive enrichment analysis.

CytoHubba was utilized to calculate and rank the node scores of DAPs within PPI networks based on three hub protein-based identification algorithms, including the degree of connectivity, Maximal Clique Centrality (MCC), and Maximum Neighborhood Component (MNC). The top 30 hub proteins identified by each algorithm were plotted using Venn diagrams to determine overlapping proteins. The top overlapping proteins within the main cluster were designated as hub proteins^{120–123}.

Pathway analysis

Pathway analysis was executed for the whole data set between the compared groups using Ingenuity Pathway Analysis (IPA) (QIAGEN Bioinformatics)¹²⁴. The proteomic data sets, which comprised UniProt identifiers, p-values, and fold changes of total identified proteins, were imported into Ingenuity Pathway Analysis (IPA) for core analysis. The core analysis was conducted with the setting of direct and indirect relationships between

molecules based on experimentally observed data, considering data sources in human databases within the Ingenuity Knowledge Base. IPA predicted potential canonical pathways of the proteins in this study, which were classified as activated or inhibited based on the Z-score, a statistical result of differential protein expression based on fold changes. Visualizing differentially affected pathways under different conditions was completed using the comparison analysis feature in IPA and hierarchical clustering. Pathways with Z score \geq 2.0 (absolute) and p < 0.05 in at least one of the conditions were considered significant and reserved for comparison. Terms were filtered with respect to functional plausibility.

Statistical analysis

Statistical analyses were conducted using GraphPad Prism software (version 8.4.3). Continuous variables were expressed as mean \pm standard deviation (SD), and categorical variables were expressed as percentages. Before statistical analysis, we assessed the normality of the data using the Shapiro–Wilk test¹²⁵. Since the p-values were greater than 0.05 (p \geq 0.05), suggesting normal distribution of the data, we employed parametric tests for the analyses. The differences in PBMC yield, purity and composition between the various PBMC isolation protocols and in CD marker expression and ratio between control and activated hPBMCs and oPBMCs were analyzed using ANOVA with Sidak correction for multiple comparisons when applicable. A two-sided Student's t test was performed to analyze differences between the unwashed PBMCs and washed PBMCs. A p-value < 0.05 was considered significant.

Ethics approval

This study was carried out using peripheral blood obtained by venipuncture from the jugular vein of six healthy adult, 3–4-year-old ewes, with ethical approval by the institutional ethics and animal welfare committee and the national authority (license BMWF-68.205/0116-V/3b/2018) and in accordance with the ARRIVE guidelines. No human participants were involved in this study; human proteomics data were retrieved from the ProteomeXchange Consortium through the proteomics identification database (PRIDE)¹⁶⁷ repository with the dataset identifier PXD001415 (https://doi.org/10.6019/PXD001415).

Results

Ovine PBMCs isolation

The oPBMCs isolation protocol was optimized regarding key variables including blood dilution, density gradient medium, and centrifugation parameters such as force and duration. Isolation protocols with blood diluted at 1:1 or 1:2 ratios in complete RPMI medium, utilizing either Lymphoprep or Ficoll for density gradient separation, and centrifuging at $660\times g$ for durations of 30 or 60 min, achieved optimal layer separation. These protocols delineated four distinct layers—erythrocyte/granulocyte, density gradient medium, PBMCs, and plasma—more effectively and without perturbation than methods using undiluted blood, Percoll as the separation medium, and centrifugation forces of $800\times g$ or $330\times g$ (Fig. 1b).

Comparison of the effect of different centrifugation durations (30 min vs 60 min at $660\times g$) and density gradients (Ficoll versus Lymphoprep) on oPBMC isolation quantity and quality, revealed a statistically significant effect of density gradient (F=34.64, DFn=1, DFd=2, p=0.0277) but not centrifugation time (F=7.681, DFn=1, DFd=2, p=0.1093) on PBMC yield with Lymphoprep providing a higher PBMC yield (Table 1, Fig. 1c). In contrast, the percentage of granulocyte contamination was statistically significantly lower following a centrifugation time of 30 versus 60 min ((F=44.67, DFn=1, DFd=2, p=0.0217) but did not differ between density gradients (F=1.762, DFn=1, DFd=2, p=0.3156) (Table 1, Fig. 1d). Equally, PBMC composition (%lymphocytes vs % monocytes) differed significantly only between the different centrifugation times (F=42.91, DFn=1, DFd=4, p=0.0028) but not between density gradients (F=0.8183, DFn=1, DFd=4, p=0.4168) (Table 1, Fig. 1d). Across all protocols, cell viability remained at 100%, as confirmed by trypan blue exclusion. Furthermore, erythrocyte contamination was minimal $(0.01-0.02\times10^6 / \mu L)$ or completely absent.

Prioritizing first the purity and then the yield of the PBMCs, the isolation technique using blood diluted 1:1 with complete RPMI medium, Lymphoprep density gradient, centrifugation at $660 \times g$ for 30 min and erythrolysis followed by two washing steps, proved most effective and was thus used for all subsequent experiments.

Proteomic validation of the purity of isolated oPBMCs

MS-based proteomic analysis enabled efficient monitoring of contaminants, namely platelets and plasma and granulocytes. Notably, the optimized isolation protocol significantly diminished the presence of platelets (F = 242.5, DFn = 1, DFd = 14, p < 0.0001) and plasma proteins (F = 471, DFn = 1, DFd = 15, p < 0.0001) in the purified PBMCs (Fig. 1e). Granulocyte contamination, evidenced by the detection of granulocyte-specific CD antigens (CD177, CD55, and Alox15) through MS-based proteomic analysis, was minimal in both washed and unwashed PBMCs (F = 0.637, DFn = 1, DFd = 15, p = 0.437, Fig. 1e). This was quantitatively confirmed using a hemocytometer, revealing a mean contamination rate of $3\% \pm 1.1\%$. Therefore, the overall purity of isolated PBMCs, assessed by MS-based proteomic and hemocytometer analyses, exceeded 95%, confirming the protocol's efficiency and reliability for various downstream applications.

Proteomic phenotypic characterization of isolated oPBMCs

MS-based proteomic analysis successfully identified 32 orthologous CD antigens with hPBMCs, categorizing PBMCs into six different immune cell subsets, encompassing both lymphocyte and myeloid cell lineages. Specifically, these subsets included CD14⁺ CD16⁺ monocytes, CD3⁺CD4⁺ T cells, CD3⁺CD8⁺ T cells, CD19⁺CD22⁺ B cells, CD11c⁺ mDCs, and CD244⁺CD352⁺ NK cells (Table 2, Fig. 1f). In addition, the proteomic analysis revealed pan-leukocyte markers, including CD74 and CD37. However, uniquely in oPBMCs, our results identified a

			Cell numb	Cell number isolated/ ml blood		tage ted
Cell type	Centrifugation time (min)	Density gradient	Mean	S.D	Mean	S.D.
PBMC total 60	20	Ficoll	3.91E+06	9.25E+05	96.4	1.9
	30	Lymphoprep	4.88E+06	6.83E+05	97.0	2.1
		Ficoll	5.34E+06	2.04E+05	91.2	2.8
	60	Lymphoprep	6.16E+06	1.77E+05	92.5	1.5
Granulocyte	30	Ficoll	1.39E+05	3.76E+04	3.6	0.7
	30	Lymphoprep	1.40E+05	3.19E+04	3.0	1.1
	60	Ficoll	4.71E+05	1.64E+05	8.8	2.8
	60	Lymphoprep	4.62E+05	2.48E+04	7.5	0.5
Managarta	20	Ficoll	2.84E+05	7.91E+04	7.2	0.6
	30	Lymphoprep	3.99E+05	1.29E+05	8.0	1.6
Monocyte		Ficoll	2.40E+05	1.76E+04	4.5	0.5
	60	Lymphoprep	3.38E+05	2.60E+04	5.5	0.5
	30	Ficoll	3.49E+06	8.21E+05	89.2	1.3
	30	Lymphoprep	4.34E+06	5.84E+05	89.0	0.5
Lymphocyte	CO	Ficoll	4.63E+06	6.17E+04	86.8	2.3
	60	Lymphoprep	5.36E+06	2.00E+05	87.0	1.0

Table 1. Comparative analysis of oPBMC isolation efficiency: impact of centrifugation duration and density gradient media on the cell number (mean \pm s.d.) isolated per ml blood and the percentage of isolated PBMCs.

WC1 $^+$ $\gamma\delta$ T cell subset characterized by T-cell receptor (TCR) gamma chain (W5Q8Z2) and WC1.1-like antigens (W5QFU9) (Fig. 1f), which were not detected in hPBMCs within our datasets.

Remarkably, the majority (21 of 32) of CD markers displayed conserved patterns of expression, exhibiting no significant differences between species and activation states (p > 0.05). In contrast, 8 (of 32) CD markers (CD8a, CD99, CD22, CD59, CD172a, CD54, CD37, and CD58), were significantly differentially expressed between humans and sheep, and 4 CD markers (CD3-Z, CD50, CD14, and CD54) were significantly influenced by activation status (p < 0.05), with one CD marker (CD54) being significantly affected by species and activation states (Table 2, Suppl. Table 1).

Analysis of the various immune cell surface marker ratios, including T-cells: monocytes (CD3:CD16, CD3:CD163), T-cells:B-cells (CD3:CD19), T-cells:natural killer cells (CD3:CD352), T-cells:dendritic cells (CD3:CD11c), and T-helper cells:T-cytotoxic cells (CD4:CD8) across ovine and human, in both healthy control and inflamed PBMCs, based on their specific CD marker expressions, revealed no significant effects of species or activation status on the overall ratio of immune cell surface markers (p>0.05). However, differential trends in specific immune cell surface marker ratios under different conditions were observed. Notably, healthy oPBMCs exhibited a 2.09 to 3.53-fold increase in the ratio of T-cell surface markers to the other PBMC surface markers compared to healthy hPBMCs, except for CD3:CD352, which was higher in humans (Table 3, Suppl. Table 2). In inflamed PBMCs, ovine CD-marker ratios for T-cells: monocytes and T-helper-cells: T-cytotoxic-cells were 2.5 to 21.5-fold higher compared to hPBMCs, respectively, while the other ratios were similar across species. (Table 3, Suppl. Table 2). Comparing the control and activated groups of PBMCs, both oPBMCs and hPBMCs showed similar patterns of either increased (CD3:CD16, CD3:CD163) or decreased (CD3:CD19, CD3:CD352) ratios. However, CD4:CD8 increased and CD3:CD11c decreased in sheep, while remaining constant in humans (Table 3, Suppl. Table 2).

Proteome profiling of inflammatory stimulated ovine and human PBMCs

Mass spectrometry (MS)-based profiling

Upon inflammatory activation of PBMCs, the MS-based proteomic analyses profiled 4217 proteins in the whole cell lysates of oPBMCs and 4574 in hPBMCs, alongside 1913 proteins in the secretome of oPBMCs and 1375 in hPBMCs. This profiling was conducted after applying stringent filters for high confidence (FDR < 0.01 at both peptide and protein levels) and reproducibility, ensuring each protein was positively identified in at least 70% of the samples from one sample group. The comparative proteomic profiling of hPBMCs and oPBMCs demonstrated a notable interspecies overlap. Specifically, 47.8% of the proteins identified in the cell lysate (equivalent to 2790 proteins) and 32.8% of the secretome (comprising 988 proteins) were shared across both species.

Shared and species-specific differentially abundant proteins

In oPBMCs, 71 proteins and in hPBMCs, 176 proteins were differentially abundant ($\mid FC \mid \geq 2$, p < 0.05). Among the 71 DAPs identified in oPBMCs, 59 were upregulated (52 in whole cell lysate, 5 in secretome and 2 in both), while 12 were downregulated (11 in whole cell lysate and 1 in secretome) (Suppl. Table 3). In hPBMCs, out of 176 DAPs, 113 were upregulated (76 in whole cell lysate, 26 in secretome and 11 in both), whereas 63 were downregulated proteins (51 in proteome, 11 in secretome and 1 in both) (Suppl. Table 4).

PBMCs cell		Human	Sheep accession	n	Human control vs activated		Sheep control vs activated		Human versus sheep control		Human vs sheep activated	
type	Gene name	accession no	no	Protein name	Mean diff	Adj. p	Mean diff	Adj. p	Mean diff	Adj. p	Mean diff	Adj. p
	CD3E	P07766	W5PGT2	T-cell surface glycoprotein CD3 epsilon chain	6.9	0.44	0.1	1.00	-12.9	0.88	-19.7	0.75
	CD3D	P04234	W5PHC2	T-cell surface glycoprotein CD3 delta chain	-6.6	0.41	-0.9	0.98	-44.2	0.19	-38.5	0.27
	CD3G	P09693	W5PHL4	T-cell surface glycoprotein CD3 gamma chain	9.2	0.14	-2.0	0.86	-33.0	0.12	-44.2	0.04*
	CD3-ZETA	P20963	W5PR78	T-cell surface glycoprotein CD3 zeta chain	-12.4	0.01*	-0.7	0.92	-30.1	0.19	-18.4	0.50
	CD4	P01730	W5P8J5	T-cell surface glycoprotein CD4	3.2	0.73	-4.4	0.56	9.5	0.38	2.0	0.96
T cell	CD8A	P01732	W5QHT2	T-cell surface glycoprotein CD8 alpha chain	-3.9	0.61	10.1	0.11	40.0	0.04*	54.0	0.01*
	CD6	P30203	W5Q3F8	T-cell differen- tiation antigen CD6	5.8	0.85	1.3	0.99	4.0	0.98	-0.6	1.00
	CD5	P06127	W5Q3P2	T-cell surface glycoprotein CD5	0.8	0.97	0.8	0.97	-23.8	0.50	-23.8	0.50
	CD45	P08575	W5Q2E5	Receptor-type tyrosine-protein phosphatase C	6.7	0.76	0.0	> 0.99	-7.9	0.98	-14.5	0.94
	CD166	Q13740	W5QBM4	CD166 antigen	- 3.9	0.92	-14.4	0.38	11.3	0.83	0.7	1.00
	CD50	P32942	W5Q306	Intercellular adhesion mol- ecule 3	6.9	0.29	13.6	0.05	22.8	0.60	29.5	0.44
	CD99	P14209	W5PED4	CD99 antigen	0.4	1.00	-8.7	0.51	-38.0	0.00*	-47.1	0.00*
	CD14	P08571	W5QJA2	Monocyte differentiation antigen CD14	21.2	0.09	10.7	0.39	48.6	0.05*	38.1	0.12
	CD163	Q86VB7	W5NY01	Scavenger receptor cysteine-rich type 1 protein M130	19.7	0.15	7.0	0.70	19.2	0.23	6.5	0.82
Monocyte	CD9	P21926	W5PFL8	CD9 antigen	4.5	0.81	7.2	0.60	-26.6	0.55	-24.0	0.61
•	CD11b	P11215	W5PGV0	Integrin alpha- M	-0.1	1.00	10.1	0.04*	1.6	1.00	11.8	0.89
	CD16a	P08637	W5PK31	Low affinity immunoglobu- lin gamma Fc region receptor III-A	20.2	0.29	12.2	0.58	14.3	0.82	6.3	0.96
	CD18	P05107	W5PS30	Integrin beta-2	0.0	>0.99	6.9	0.40	3.8	0.99	10.6	0.91
	CD19	P15391	W5NUF5	B-lymphocyte antigen CD19	-3.9	0.89	-24.2	0.09	17.3	0.25	-2.9	0.95
B cell	CD22	P20273	W5P3Y9	CD22 molecule	2.7	0.94	-8.8	0.57	-32.8	0.00*	-44.4	0.00*
	CD180	Q99467	W5P7C7	CD180 antigen	-3.7	0.91	-3.6	0.92	3.4	0.97	3.6	0.97
	CD352	Q96DU3	W5PGE8	SLAM family member 6	-3.8	0.93	-3.3	0.94	-26.5	0.23	-26.1	0.24
Natural Killer	CD244	Q9BZW8	W5PGV6	Natural killer cell receptor 2B4	2.2	0.54	2.0	0.59	11.7	0.16	11.5	0.17
	CD59	P13987	W5Q927	CD59 glyco- protein	-9.1	0.36	-2.5	0.91	-46.0	0.02*	- 39.4	0.05*
	CD11c	P20702	W5PH85	Integrin alpha-X	8.1	0.28	- 5.9	0.47	27.7	0.67	13.7	0.90
Dendritic cells	CD172a	P78324	W5PVB4	Tyrosine-pro- tein phosphatase non-receptor type substrate 1	13.2	0.02*	-7.0	0.11	-4.5	0.53	-24.7	0.00*
	CD54	P05362	W5Q263	Intercellular adhesion mol- ecule 1	-9.6	0.08	-43.2	0.00*	51.5	0.00*	17.8	0.23

PBMCs cell		Human	Sheep accession		Human con activated	trol vs	Sheep contractivated	ol vs	Human ver	sus sheep	Human vs s activated	heep
type	Gene name	accession no		Protein name	Mean diff	Adj. p	Mean diff	Adj. p	Mean diff	Adj. p	Mean diff	Adj. p
	CD74	P04233	W5PBE0	HLA class II histocompat- ibility antigen gamma chain	5.0	0.63	-13.8	0.11	-29.5	0.46	-48.3	0.17
	CD37	P11049	W5PTI0	Leukocyte antigen CD37	27.5	0.11	-3.6	0.94	-17.9	0.31	-49.0	0.01*
Leukocyte	CD47	Q08722	W5QC22	Leukocyte surface antigen CD47	-4.3	0.39	-3.1	0.59	17.3	0.56	18.6	0.51
	CD44	P16070	W5QBV7	CD44 antigen	- 3.9	0.78	-4.4	0.73	16.5	0.73	15.9	0.74
	CD58	P19256	W5QG77	Lymphocyte function-associ- ated antigen 3	0.0	> 0.99	-4.4	0.79	-65.0	< 0.00*	-69.3	< 0.00*

Table 2. Comparison of CD marker expression between ovine and human control and activated PBMCs (*indicates p < 0.05).

PBMCs cell type		T cell: monocyte	T cell: monocyte	T cell: DC	T cell: B cell	T cell: NK cell	Thelper: tcytotoxic
CD group	Item	CD3:CD16	CD3:CD163	CD3E:CD11c	CD3:CD19	CD3:CD352	CD4:CD8
** 1	Fraction	1.85	2.13	1.00	1.90	4.02	0.81
Human control	Ratio	1:0.54	1:0.47	1:1.00	1:0.53	1:0.25	1:1.24
Chase soutual	Fraction	3.87	7.53	2.17	4.85	1.79	2.61
Sheep control	Ratio	1:0.26	1:0.13	1:0.46	1:0.21	1:0.56	1:0.38
**	Fraction	4.11	5.83	1.02	1.51	2.88	0.70
Human activated	Ratio	1:0.24	1:0.17	1:0.98	1:0.66	1:0.35	1:1.44
Charmantinatad	Fraction	10.41	25.15	1.85	1.89	1.66	14.96
Sheep activated	Ratio	1:0.1	1:0.04	1:0.54	1:0.53	1:0.60	1:0.07
ANOVA amarica	F (Dfn, Dfd)	F (1, 4) = 0.01	F(1, 4) = 0.9	F (1, 4) = 4.92	F (1, 4) = 0.32	F (1, 4) = 0.05	F(1, 4) = 0.25
ANOVA species	p value	0.92	0.39	0.09	0.60	0.83	0.64
ANOVA activation	F (Dfn, Dfd)	F(1,4)=0.02	F(1, 4) = 0.75	F (1, 4) = 2.56	F (1, 4) = 0.33	F(1,4)=0.06	F (1, 4) = 1.23
status	p value	0.89	0.44	0.18	0.60	0.82	0.33

Table 3. Comparison of surface marker ratios across species and activation states.

Venn analysis, capturing the overlap between 176 and 71 DAPs in human and sheep PBMCs, identified 7 overlapped DAPs (IL1B, IFIH1, CCL4, ISG20, IL1RN, APOBEC3A, and PDCD11), which were simultaneously associated with human and sheep activated PBMCs, as well as 169 human-specific DAPs (107 upregulated and 62 downregulated), and 64 sheep-specific DAPs (52 upregulated and 12 downregulated) (Fig. 2). The top 10 DAPs of activated PBMCs in humans and sheep are listed in Table 4.

Enrichment analyses

DAPs of activated PBMCs were significantly enriched in 68 GO terms in sheep and 310 GO terms in humans (FDR < 0.05), of which 16 were shared between ovine and human PBMCs, 52 were ovine-specific and 294 human-specific (Suppl. Tables 5–7).

The shared biological process ontologies of DAPs included defense response, response to stress, immune response, defense response to virus, defense response to other organism, Inflammatory response, cellular response, interspecies interaction between organisms, response to other organism, innate immune response, and immune effector process. Molecular function ontology of DAPs was associated with protein binding, RNA helicase activity, and binding (Suppl. Table 7).

Enrichment analysis using KEGG pathways revealed 5 shared key pathway categories between ovine and human DAPs, including NF-kappa B signaling pathway, IL-17 signaling pathway, TNF signaling pathway, cytosolic DNA-sensing pathway, and cytokine-cytokine receptor interaction (FDR < 0.001, Suppl. Table 7).

Protein-protein-interaction network construction and module analysis

Protein–protein interaction (PPI) networks for DAPs of oPBMCs revealed 71 nodes, 219 edges vs. 73 expected edges (clustering coefficient: 0.475, enrichment p-value: 1.0E–16, average node degree: 6.17). In contrast, hPBMCs exhibited 168 nodes, 684 edges vs. 203 expected edges (clustering coefficient: 0.496, enrichment p-value: 1.0E–16, average node degree: 8.14). Furthermore, protein complex analysis of MCODE identified three clusters within the sheep PPI network, totally including 22 nodes and 74 edges (Fig. 3a, Suppl. Table 8), and

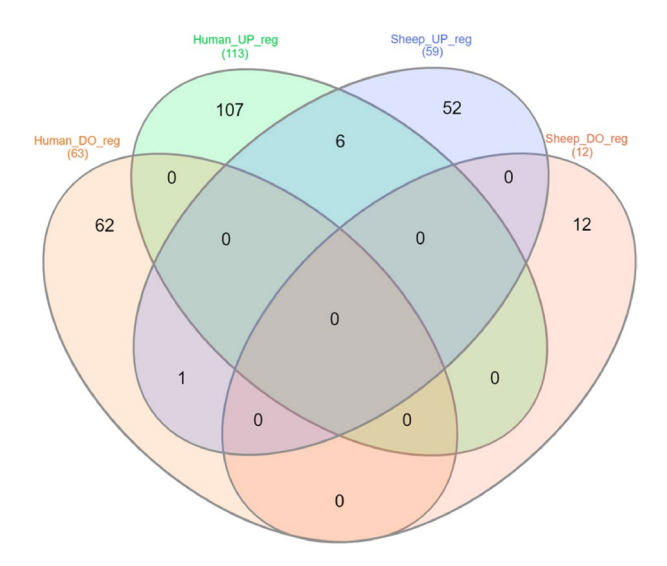


Figure 2. Comparative Venn analysis of differential abundant proteins (DAPs) in ovine vs. human peripheral blood mononuclear cells (PBMCs). Venn analysis of DAPs (fold change $|\geq 2|$, p<0.05) that were upregulated (UP_reg) or downregulated (DO_reg) in response to inflammation in ovine and human PBMCs, yielded 6 overlapping upregulated DAPs (IL1B, IFIH1, CCL4, ISG20, IL1RN, and APOBEC3A) and 1 overlapping downregulated DAP (PDCD11), while the remainder of the DAPs were species-specific.

Species	Gene name	Accession no.	Protein name	p-value	Fold CHANGE	Subcellular location
	STAT3	W5NTT2	Signal transducer and activator of transcription	1.98E-02	2.14	Cell lysate
	IL1B	M4WG34	Interleukin-1 beta	1.33E-03	2.76	Secretome
	ILIB	M4WG34	Interieukin-1 beta	5.71E-03	2.71	Cell lysate
	IRF4	W5P0Y0	Interferon regulatory factor 4	2.30E-03	2.74	Cell lysate
	IFIH1	W5P825	RNA helicase	2.15E-02	2.70	Cell lysate
Ovine	IL17F	W5PXB0	Interleukin 17F	4.21E-03	2.69	Secretome
	TNFAIP3	W5NQZ0	Ubiquitinyl hydrolase 1	2.26E-02	2.65	Cell lysate
	IL17A	W5PWW6	Interleukin-17a	4.72E-03	2.60	Secretome
	SATB1	W5Q210	DNA-binding protein SATB	3.07E-03	2.60	Cell lysate
	STAT1	C8BKE1	Signal transducer and activator of transcription	5.42E-03	2.49	Cell lysate
	CCL4	W5P2A3	C-C motif chemokine	2.68E-02	2.21	Secretome
	IL6	P05231	Interleukin-6	1.65E-07	8.65	Secretome
	ILO	P05251	Interieukin-6	2.53E-04	4.45	Cell lysate
	IL1B	P01584	Interleukin-1 beta	3.71E-08	8.05	Secretome
	ILIB	F01364	Interieukiii-1 beta	3.31E-05	4.20	Cell lysate
	IFIT3	O14879	Interferon-induced protein with tetratricopep-	5.30E-07	7.54	Cell lysate
	11113	014879	tide repeats 3	3.21E-03	3.99	Secretome
	CCL2	P13500	C-C motif chemokine 2	1.37E-06	7.52	Secretome
	IL1A	P01583	Interleukin-1 alpha	1.54E-06	7.26	Cell lysate
Human	ILIA	P01585	тпенецкіп-т агрпа	5.14E-04	3.40	Secretome
	IFIH1	Q9BYX4	Interferon-induced helicase C domain-containing protein 1	2.49E-04	6.77	Cell lysate
	CCL3	P10147	C–C motif chemokine 3	3.56E-04	6.19	Secretome
	CCLS	P10147	C-C moth chemokine 3	7.38E-04	4.08	Cell lysate
	CSPG2	P13611	Versican core protein	5.88E-07	- 5.64	Secretome
	ISG15	D05161	IThis witting like mantain ICC15	4.91E-04	5.33	Cell lysate
	18G15	P05161	Ubiquitin-like protein ISG15	1.27E-03	4.28	Secretome
	IFIT1	P09914	Interferon-induced protein with tetratricopeptide repeats 1	1.81E-04	4.95	Cell lysate

Table 4. Top 10 differentially abundant proteins in activated vs. control PBMCs in sheep and human (Fold Change $\mid \geq 2 \mid$, p<0.05). Proteins detected in both secretome and whole cell lysate datasets are highlighted in bold.

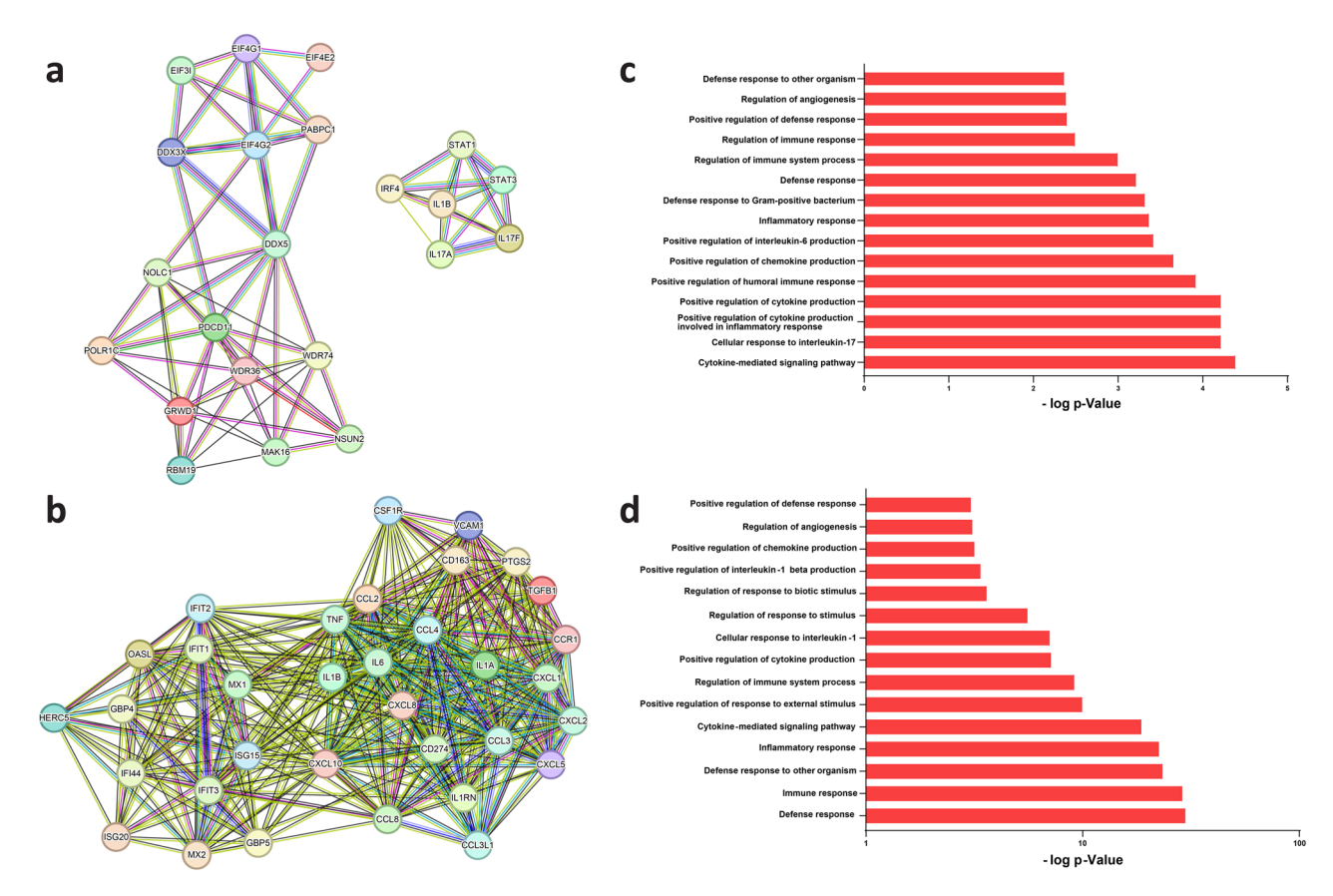


Figure 3. Comparative protein–protein interaction (PPI) networks and functional enrichment in ovine and human PBMCs, showing (a) the ovine main PPI cluster, (b) the human main PPI cluster, (c) functional enrichment of biological processes in ovine differentially abundant proteins (DAPs) and (d) functional enrichment of biological processes in human DAPs.

one cluster within the human PPI network, totally including 34 nodes and 316 edges (Fig. 3b, Suppl. Table 8). The first and the second clusters in sheep were associated with RNA metabolism, and regulation of translational initiation (Suppl. Table 9). The third cluster in sheep, including six DAPs, and the primary cluster in human, including 34 DAPs, were predominantly associated with inflammatory responses. In the main cluster of DAPs 45 GO terms related to inflammatory biological processes were significantly enriched (FDR < 0.05) in sheep and 324 GO terms in humans (Suppl. Tables 9, 10). Within this set, 29 biological process terms were shared between the main clusters of sheep and human PBMCs (Suppl. Table 11), while 16 were specific to sheep and 295 were specific to humans. The top 15 biological process terms within the main cluster of PBMCs in humans and sheep are shown in Fig. 3c,d.

Venn analysis, capturing the overlap between three CytoHubba algorithms, identified 27 overlapped proteins for sheep and 28 for humans. Subsequently, the top overlapped proteins within the main cluster were designated as hub proteins. Within the main ovine cluster, the hub proteins were STAT1, IL1B, IRF4, STAT3, and IL17A, while in the main human cluster, they were CXCL10, CXCL8, IL1B, IL6, and TNF (Suppl. Tables 12–14). Remarkably, these hub proteins were identified as species-specific, with IL1B being the sole hub protein shared between activated PBMCs during the 6-h time course in both humans and sheep. Enrichment analysis confirmed the relevance of these hub proteins to inflammatory responses in both species.

Pathway analyses

Ingenuity pathway analysis of the differential proteomic expression profiles of hPBMCs secretome, oPBMCs secretome, hPBMCs whole cell lysate, and oPBMCs whole cell lysate, identified 17 canonical pathways that exhibited conserved activation/inhibition patterns across both species. Additionally, seven canonical pathways demonstrated divergent activation/inhibition patterns between both species (Table 5).

The top 5 cross-species conserved pathways that were activated in the secretome and whole cell lysate, were interferon signaling, inflammasome pathway, Pathogen Induced Cytokine Storm Signaling Pathway, NOD1/2 Signaling Pathway, and acute phase response signaling (Table 5). The top 5 cross-species pathways that were activated in the secretome and then inactivated at the level of the whole cell lysate in both species, were phagosome formation, CXCR4 signaling, IL-8 signaling, NF- κ B Activation by viruses, and ERK/MAPK Signaling (Table 5).

The top 5 pathways with a species-specific activation pattern, that were activated in the secretome of both species but inactivated at the level of the whole cell lysate only in sheep, were IL-6 signaling, IL-17 signaling, p38 MAPK signaling, HMGB1 Signaling, and S100 Family Signaling Pathway (Table 5).

Canonical pathways	HSE	SSE	HCL	SCL
Conserved activation patterns				
Role of hypercytokinemia/hyperchemokinemia in the pathogenesis of influenza	4.1	2.6	3.5	3.0
Interferon signaling	2.6	1.0	1.5	2.1
Autophagy	2.2	1.7	0.6	1.8
Inflammasome pathway	2.0	2.0	0.8	1.4
Acute phase response signaling	2.1	3.3	1.9	0.9
Ceramide signaling	1.2	2.1	1.5	1.2
NOD1/2 signaling pathway	2.8	1.0	0.7	0.6
Pathogen induced cytokine storm signaling pathway	2.3	1.8	0.9	0.8
Conserved inhibition patterns				
Serotonin receptor signaling	3.6	3.8	-0.9	-1.2
Phagosome formation	1.6	1.5	-2.2	-2.2
Integrin signaling	1.4	1.2	-1.3	-3.2
NF-κB activation by viruses	2.2	0.9	-0.3	-0.5
Role of PI3K/AKT signaling in the pathogenesis of influenza	2.0	1.1	-0.7	-0.7
ERK/MAPK signaling	2.3	2.3	-0.3	-2.4
IL-33 signaling pathway	2.7	1.5	-0.4	-0.5
CXCR4 signaling	2.5	1.4	-1.2	-0.5
IL-8 signaling	2.3	2.6	-1.8	-1.6
Divergent activation patterns		•		
HMGB1 signaling	4.6	1.7	0.8	-0.4
Mitochondrial dysfunction	1.7	-2.2	-1.9	-3.2
Glycolysis I	1.1	1.1	1.6	- 2.1
IL-6 signaling	2.4	2.3	1.5	-1.3
p38 MAPK signaling	2.5	1.3	1.3	-0.4
S100 family signaling pathway	2.6	1.8	0.9	-1.1
IL-17 signaling	2.5	1.1	0.9	-0.5

Table 5. Comparative analysis of canonical pathways in human and ovine PBMCs based on differential proteomic expression across secretome (*HSE* human PBMC secretome, *SSE* ovine PBMC secretome) and whole cell lysate (*HCL* human PBMC whole cell lysate, *SCL* ovine PBMC whole cell lysate) datasets.

Discussion

Sheep are commonly employed as a large animal model in immune-related studies^{62,66,67,70}. However, inherent differences between human and sheep PBMCs may impact the translational relevance of research findings derived from sheep models. Therefore, in this cross-species comparative study, we examined the similarities and differences of the in vitro inflammatory response of ovine and human PBMCs by employing mass spectrometry to analyze the proteome of the PBMCs' secretome and whole cell lysate.

The proteomic phenotyping of human and ovine PBMCs revealed 32 orthologous CD antigens with no significant difference in abundance levels between species. The surface markers indicated the presence of six distinct immune cell subsets in both human and ovine PBMCs, CD14+ CD16+monocytes, CD3+CD4+ T cells, CD3+CD8+ T cells, CD19+CD22+ B cells, CD11c+ mDCs, and CD244+CD352+ NK cells, consistent with established classifications $^{63,126-128}$. However, ovine PMBCs also contained a unique WC1+ $\gamma\delta$ T cell subset, not detected in hPBMCs. While the comparable abundance levels of immune cell subset markers indicate a similar composition of ovine and human PBMCs, establishing a crucial foundation for modeling inflammatory responses and interpreting subsequent proteomic shifts in both species, the presence of a unique T-cell subset introduces a potential confounding species-specific difference.

Comparative proteomic profiling of hPBMCs and oPBMCs revealed an overlap of approximately half (47.8%, 2790 proteins) of the entire cell lysate proteome, and one-third (32.8%, 988 proteins) of the secretome proteome between the two species. However, upon inflammatory stimulation, only seven differentially abundant proteins (IL1B, IFIH1, CCL4, ISG20, IL1RN, APOBEC3A, and PDCD11) were shared between sheep and humans, while 169 were specific to humans and 64 species-specific to sheep. This limited overlap, although consistent with comparable studies exploring proteome/transcriptome changes in human and mouse during Th17 cell differentiation 129,130, is even more pronounced at the protein level of PBMCs in the current study. Two primary factors may contribute to this lack of overlap. First, considerable heterogeneity and compositional variations exist among circulating PBMCs in different species 50,131,132 . For instance, $\gamma\delta$ T cells, a subset of lymphoid cells, typically constitute 0.5–10% of circulating T lymphocytes in adult humans 132,133 , while in adult sheep they represent up to $17\%^{131,133}$ and in lambs $30-60\%^{134-137}$. This heterogeneity may explain the successful identification of CD markers specific to the WC1 $^+$ $\gamma\delta$ T cell subset in oPBMCs, a subset not detected in our hPBMCs samples. Second, inter-species differences in the cellular machinery arise from the intricate interplay between the

conservation and diversification of regulatory mechanisms^{87,138}. Therefore, incorporating signals not only at the level of orthologous individual molecules (proteins) but also within functional sets, complexes, and pathways is crucial when translating findings from ovine immunology to the human setting.

Using PPI networks and GO analyses, we identified 16 shared GO terms between both species with a strong representation of inflammatory-related processes. Enrichment analysis identified the major shared biological process "immune and inflammatory responses", encompassing high-enrichment terms such as "leukocyte activation", "leukocyte migration", "leukocyte degranulation", "leukocyte-mediated immunity", "adaptive immune response", "innate immune response", and "cytokine production involved in immune response" that are associated with well-established consequences of inflammatory activation of PBMCs by LPS/PHA \$5,107,140.

Network analysis revealed five potential hub proteins in sheep and humans, primarily associated with inflammatory processes 55,98,101,141,142. In sheep, the hub proteins included STAT1, IL1B, IRF4, STAT3, and IL17A, while in humans, they comprised CXCL10, CXCL8, IL1B, IL6, and TNF. Notably, IL1B, a potent pro-inflammatory cytokine with a pivotal role in orchestrating innate and adaptive immune responses 143,144, emerged as the sole hub protein shared between both species, detected in the whole cell lysates and secretomes of PBMCs.

Considering that the secretome samples and the cell lysate samples were collected simultaneously, the obtained secretomes contain accumulated proteins synthesized and secreted over the incubation time (6 h in the current study), whereas the proteins obtained from the cell lysates give insight in the current cell status at the time point of collection. The current study utilized integrative global mass spectrometry-based proteomics analyses of both the secretome (extracellular) and whole cell lysate (intracellular) of PBMCs to assess of the pattern of activation/ inhibition in shared signaling pathways and their underlying molecular mechanisms across both species and gain insight into the intricate regulatory mechanisms. In response to inflammatory stimulation, 17 canonical pathways, associated with the DAP of PBMCs of both species, exhibited consistent trends of activation/inhibition in both the secretome and the cell lysates (e.g., interferon signaling, inflammasome pathway, Pathogen Induced Cytokine Storm Signaling Pathway, acute phase response signaling, ERK/MAPK Signaling, CXCR4 Signaling, NF-κB Activation by Viruses, IL-33 Signaling, IL-8 Signaling, Integrin Signaling, etc.), emphasizing a high degree of conservation in immune and inflammatory responses across species. This observed conservation can be attributed to the substantial evolutionary conservation of inflammatory signaling and its transcriptional mechanisms in vertebrates^{145,146}, despite variations in susceptibility and physiological differences between species^{147–150}. For instance, the substantial homology between ovine and human Toll-like receptors (82-88% homology)^{151,152}, as well as the close similarity in genomic responses and cardiopulmonary hemodynamics of sheep and humans challenged with lipopolysaccharide (LPS), further support the conservation^{70,152–158}.

However, 7 divergent canonical pathways exhibited different trends of activation/inhibition in humans and sheep highlighting potential species-specific adaptive differences in the regulation of intracellular signaling pathways. Specifically, initial activation of "IL-6 signaling", "HMGB1 signaling", "p38 MAPK signaling", "S100 family signaling pathway", "IL-17 signaling", "Mitochondrial Dysfunction", and "Glycolysis I" was evident in the secretome of both species but rapid inhibition only in the whole cell lysate of sheep. These finding align with previous studies suggesting that differences in chemokine and cytokine expression and the response of various cell types to inflammatory cytokines across species might be related to species variability in regulation of inflammatory signaling pathways^{70,159–161}. Inflammatory pathways are finely tuned by interconnected activating and inhibitory waves that delicately adjust the magnitude and duration of the inflammatory response over time to prevent tissue damage^{162–165}. Thus, considering temporal changes in pathway regulation^{163,166–168} is crucial when translating pathways between sheep models and humans in future studies.

The lack of traditional immunochemical validation assays, primarily due to scarce sheep-specific antibodies, presents a methodological limitation of this study. However, Mass Spectrometry proteomics provides indirect validation by detecting proteomic patterns that are consistent with previously validated research 49,51-53,140,169-173. Additionally, the MS-data provide a foundation for further refinement of the design of specific ovine antibodies for immuno-based analytical methods in future studies investigating immune repertoires in health and disease.

In conclusion, this cross-species comparative proteomics study sheds light on the intricate differences and shared aspects of the in vitro inflammatory response in ovine and human PBMCs, underscoring the importance of a judicious model selection to optimize the translatability of findings and uphold ethical standards in research. While significant similarities were found in conserved inflammatory pathways and biological processes, recognizing and addressing inherent species-specific differences is imperative when interpreting results of inflammation research results conducted in the ovine model. For inflammatory processes exhibiting divergence between the two species, the utilization of human-derived in vitro models or alternative animal models is recommended to optimize translational potential. Evidence-based selection of fit-for-purpose models ensures scientific quality and relevance of pre-clinical inflammation research while minimizing unnecessary animal use.

Data availability

The datasets generated and analysed during the current study are included in this published article (and its Supplementary Information files) or available from the corresponding author on reasonable request.

Received: 23 March 2024; Accepted: 26 June 2024 Published online: 28 June 2024

References

- Gupta, S. C., Kunnumakkara, A. B., Aggarwal, S. & Aggarwal, B. B. Inflammation, a double-edge sword for cancer and other age-related diseases. Front. Immunol. 9, 2160 (2018).
- 2. Roth, G. A. *et al.* Global, regional, and national age-sex-specific mortality for 282 causes of death in 195 countries and territories, 1980–2017: A systematic analysis for the Global Burden of Disease Study 2017. *Lancet* 392, 1736–1788 (2018).

- 3. Furman, D. et al. Chronic inflammation in the etiology of disease across the life span. Nat. Med. 25, 1822-1832 (2019).
- 4. Okin, D. & Medzhitov, R. Evolution of inflammatory diseases. Curr. Biol. 22, R733-R740 (2012).
- 5. Slavich, G. M. Understanding inflammation, its regulation, and relevance for health: A top scientific and public priority. *Brain Behav. Immun.* 45, 13–14 (2015).
- 6. Rock, K. L., Latz, E., Ontiveros, F. & Kono, H. The sterile inflammatory response. Annu. Rev. Immunol. 28, 321-342 (2010).
- 7. Medzhitov, R. The spectrum of inflammatory responses. Science 374, 1070–1075 (2021).
- 8. Kotas, M. E. & Medzhitov, R. Homeostasis, inflammation, and disease susceptibility. Cell 160, 816-827 (2015).
- 9. Netea, M. G. et al. A guiding map for inflammation. Nat. Immunol. 18, 826-831 (2017).
- Zindel, J. & Kubes, P. DAMPs, PAMPs, and LAMPs in immunity and sterile inflammation. Annu. Rev. Pathol. Mech. Dis. 15, 1–26 (2019).
- 11. Zhao, H. et al. Inflammation and tumor progression: Signaling pathways and targeted intervention. Signal Transduct. Target. Ther. 6, 263 (2021).
- 12. Medzhitov, R. Origin and physiological roles of inflammation. Nature 454, 428-435 (2008).
- 13. Leiba, J. et al. Molecular actors of inflammation and their signaling pathways: Mechanistic insights from zebrafish. Biology 12, 153 (2023).
- 14. Hagemann, T., Balkwill, F. & Lawrence, T. Inflammation and cancer: A double-edged sword. Cancer Cell 12, 300-301 (2007).
- 15. Chovatiya, R. & Medzhitov, R. Stress, inflammation, and defense of homeostasis. Mol. Cell 54, 281-288 (2014).
- Silva, M. T. When two is better than one: Macrophages and neutrophils work in concert in innate immunity as complementary and cooperative partners of a myeloid phagocyte system. J. Leukoc. Biol. 87, 93–106 (2010).
- 17. Silva, M. T. Macrophage phagocytosis of neutrophils at inflammatory/infectious foci: A cooperative mechanism in the control of infection and infectious inflammation. *J. Leukoc. Biol.* **89**, 675–683 (2011).
- Fullerton, J. N. & Gilroy, D. W. Resolution of inflammation: A new therapeutic frontier. Nat. Rev. Drug Discov. 15, 551–567 (2016).
- 19. Serhan, C. N. & Savill, J. Resolution of inflammation: The beginning programs the end. Nat. Immunol. 6, 1191-1197 (2005).
- 20. Sugimoto, M. A., Sousa, L. P., Pinho, V., Perretti, M. & Teixeira, M. M. Resolution of inflammation: What controls its onset? Front. Immunol. 7, 160 (2016).
- 21. Ortega-Gómez, A., Perretti, M. & Soehnlein, O. Resolution of inflammation: An integrated view. *EMBO Mol. Med.* **5**, 661–674 (2013).
- Schindler, L. et al. Macrophage migration inhibitory factor inhibits neutrophil apoptosis by inducing cytokine release from mononuclear cells. J. Leukoc. Biol. 110, 893–905 (2021).
- 23. Poon, I. K. H., Lucas, C. D., Rossi, A. G. & Ravichandran, K. S. Apoptotic cell clearance: Basic biology and therapeutic potential. Nat. Rev. Immunol. 14, 166–180 (2014).
- 24. Serhan, C. N., Chiang, N. & Dalli, J. The resolution code of acute inflammation: Novel pro-resolving lipid mediators in resolution. Semin. Immunol. 27, 200–215 (2015).
- Perretti, M. The resolution of inflammation: New mechanisms in patho-physiology open opportunities for pharmacology. Semin. Immunol. 27, 145–148 (2015).
- 26. Headland, S. E. & Norling, L. V. The resolution of inflammation: Principles and challenges. Semin. Immunol. 27, 149-160 (2015).
- 27. Gilroy, D. & Maeyer, R. D. New insights into the resolution of inflammation. Semin. Immunol. 27, 161-168 (2015).
- 28. Crean, D. & Godson, C. Specialised lipid mediators and their targets. Semin. Immunol. 27, 169-176 (2015).
- 29. Colgan, S. P. Neutrophils and inflammatory resolution in the mucosa. Semin. Immunol. 27, 177-183 (2015).
- 30. Viola, J. & Soehnlein, O. Atherosclerosis—A matter of unresolved inflammation. Semin. Immunol. 27, 184-193 (2015).
- 31. Haworth, O. & Buckley, C. D. Pathways involved in the resolution of inflammatory joint disease. *Semin. Immunol.* 27, 194–199 (2015).
- 32. Wallace, J. L., Ianaro, A., Flannigan, K. L. & Cirino, G. Gaseous mediators in resolution of inflammation. Semin. Immunol. 27, 227–233 (2015).
- 33. Nathan, C. & Ding, A. Nonresolving inflammation. Cell 140, 871–882 (2010).
- 34. Margraf, A. & Perretti, M. Immune cell plasticity in inflammation: Insights into description and regulation of immune cell phenotypes. *Cells* 11, 1824 (2022).
- 35. Calder, P. C. *et al.* A consideration of biomarkers to be used for evaluation of inflammation in human nutritional studies. *Br. J. Nutr.* **109.** S1–S34 (2013).
- 36. Liu, C. et al. Cytokines: From clinical significance to quantification. Adv. Sci. 8, 2004433 (2021).
- 37. Krenytska, D. et al. Circulating levels of inflammatory cytokines and angiogenesis-related growth factors in patients with osteoarthritis after COVID-19. Front. Med. 10, 1168487 (2023).
- 38. Kany, S., Vollrath, J. T. & Relja, B. Cytokines in inflammatory disease. Int. J. Mol. Sci. 20, 6008 (2019).
- Pan, W., Wang, Q. & Chen, Q. The cytokine network involved in the host immune response to periodontitis. Int. J. Oral Sci. 11, 30 (2019).
- 40. Ngo, L. & Tate, M. L. K. A spike in circulating cytokines TNF- α and TGF- β alters barrier function between vascular and musculoskeletal tissues. *Sci. Rep.* 13, 9119 (2023).
- 41. Sullivan, K. E. et al. Measurement of cytokine secretion, intracellular protein expression, and mrna in resting and stimulated peripheral blood mononuclear cells. Clin. Diagn. Lab. Immunol. 7, 920–924 (2000).
- van Dooren, F. H., Duijvis, N. W. & Velde, A. A. Analysis of cytokines and chemokines produced by whole blood, peripheral mononuclear and polymorphonuclear cells. J. Immunol. Methods 396, 128–133 (2013).
- Alexovič, M., Uličná, C., Sabo, J. & Davalieva, K. Human peripheral blood mononuclear cells as a valuable source of diseaserelated biomarkers: Evidence from comparative proteomics studies. *Proteom. Clin. Appl.* https://doi.org/10.1002/prca.20230 0072 (2023).
- 44. Wagar, L. E., DiFazio, R. M. & Davis, M. M. Advanced model systems and tools for basic and translational human immunology. *Genome Med.* 10, 73 (2018).
- 45. Reale, M. et al. Peripheral cytokines profile in Parkinson's disease. Brain Behav. Immun. 23, 55-63 (2009).
- Sen, P., Kemppainen, E. & Órešič, M. Perspectives on systems modeling of human peripheral blood mononuclear cells. Front. Mol. Biosci. 4, 96 (2018).
- 47. Zhang, X. *et al.* Peripheral blood mononuclear cells show prominent gene expression by erythroid progenitors in diseases characterized by heightened erythropoiesis. *Br. J. Haematol.* **190**, e42–e45 (2020).
- 48. Dobrovolskaia, M. A. & Afonin, K. A. Use of human peripheral blood mononuclear cells to define immunological properties of nucleic acid nanoparticles. *Nat. Protoc.* **15**, 3678–3698 (2020).
- 49. Alexovič, M. et al. Human peripheral blood mononuclear cells: A review of recent proteomic applications. *Proteomics* 22, 2200026 (2022).
- Li, Z. et al. Molecular mechanisms governing circulating immune cell heterogeneity across different species revealed by singlecell sequencing. Clin. Transl. Med. 12, e689 (2022).
- 51. Končarević, S. *et al.* In-depth profiling of the peripheral blood mononuclear cells proteome for clinical blood proteomics. *Int. J. Proteom.* **2014**, 129259 (2014).

- 52. Derbois, C., Palomares, M.-A., Deleuze, J.-F., Cabannes, E. & Bonnet, E. Single cell transcriptome sequencing of stimulated and frozen human peripheral blood mononuclear cells. *Sci. Data* 10, 433 (2023).
- Ngkelo, A., Meja, K., Yeadon, M., Adcock, I. & Kirkham, P. A. LPS induced inflammatory responses in human peripheral blood mononuclear cells is mediated through NOX4 and Giα dependent PI-3kinase signalling. J. Inflamm. 9, 1 (2012).
- Patel, R. S., Tomlinson, J. E., Divers, T. J., de Walle, G. R. V. & Rosenberg, B. R. Single-cell resolution landscape of equine peripheral blood mononuclear cells reveals diverse cell types including T-bet+ B cells. BMC Biol. 19, 13 (2021).
- Lin, Z. et al. Functional differences and similarities in activated peripheral blood mononuclear cells by lipopolysaccharide or phytohemagglutinin stimulation between human and cynomolgus monkeys. Ann. Transl. Med. 9, 257–257 (2021).
- Pathak, D., Srivastava, A. K., Padma, M. V., Gulati, S. & Rajeswari, M. R. Quantitative proteomic and network analysis of differentially expressed proteins in PBMC of Friedreich's ataxia (FRDA) patients. Front. Neurosci. 13, 1054 (2019).
- 57. Zhang, M. & Huang, B. The multi-differentiation potential of peripheral blood mononuclear cells. Stem Cell Res. Ther. 3, 48 (2012).
- 58. Wilk, A. J. et al. A single-cell atlas of the peripheral immune response in patients with severe COVID-19. Nat. Med. 26, 1070–1076 (2020).
- Gros, A. et al. Prospective identification of neoantigen-specific lymphocytes in the peripheral blood of melanoma patients. Nat. Med. 22, 433–438 (2016).
- 50. Christopher, M. M. One health, one literature: Weaving together veterinary and medical research. Sci. Transl. Med. 7, 303 (2015).
- Nalubamba, K. S., Gossner, A. G., Dalziel, R. G. & Hopkins, J. Differential expression of pattern recognition receptors in sheep tissues and leukocyte subsets. Vet. Immunol. Immunopathol. 118, 252–262 (2007).
- 62. Entrican, G., Wattegedera, S. R. & Griffiths, D. J. Exploiting ovine immunology to improve the relevance of biomedical models. *Mol. Immunol.* **66**, 68–77 (2015).
- Melzi, E., Rocchi, M. S., Entrican, G., Caporale, M. & Palmarini, M. Immunophenotyping of sheep paraffin-embedded peripheral lymph nodes. Front. Immunol. 9, 2892 (2018).
- Newman, E., Turner, A. S. & Wark, J. D. The potential of sheep for the study of osteopenia: Current status and comparison with other animal models. *Bone* 16, 277–284 (1995).
- 65. Taylor, W. R. et al. Tibio-femoral joint contact forces in sheep. J. Biomech. 39, 791-798 (2006).
- Hein, W. R. & Griebel, P. J. A road less travelled: Large animal models in immunological research. Nat. Rev. Immunol. 3, 79–84 (2003).
- 67. Wani, S. A. et al. Proteome modulation in peripheral blood mononuclear cells of Peste des Petits ruminants vaccinated goats and sheep. Front. Vet. Sci. 8, 670968 (2021).
- 68. Gerdts, V. et al. Large animal models for vaccine development and testing. ILAR J. 56, 53-62 (2015).
- Banstola, A. & Reynolds, J. N. J. The sheep as a large animal model for the investigation and treatment of human disorders. Biology 11, 1251 (2022).
- Enkhbaatar, P. et al. Comparison of gene expression by sheep and human blood stimulated with the TLR4 agonists lipopolysaccharide and monophosphoryl lipid A. PLoS ONE 10, e0144345 (2015).
- 71. Hessler, M. *et al.* Differential effects of selective and nonselective potassium channel inhibitors in ovine endotoxemic shock (macrocirculation) and in a rat model of septic shock (microcirculation). *Shock* **51**, 247–255 (2019).
- Modine, T., Ali, W. B. & Perrin, N. Large animal models for transcatheter heart valve prosthesis development making sheep's eyes at supra-annular banding. JACC Basic Transl. Sci. 7, 496–497 (2022).
- Hunka, J., Riley, J. T. & Debes, G. F. Approaches to overcome flow cytometry limitations in the analysis of cells from veterinary relevant species. BMC Vet. Res. 16, 83 (2020).
- 74. Meissner, F. & Mann, M. Quantitative shotgun proteomics: Considerations for a high-quality workflow in immunology. *Nat. Immunol.* 15, 112–117 (2014).
- 75. Mareddy, S., Broadbent, J., Crawford, R. & Xiao, Y. Proteomic profiling of distinct clonal populations of bone marrow mesenchymal stem cells. *J. Cell. Biochem.* **106**, 776–786 (2009).
- 76. Niehage, C. et al. The cell surface proteome of human mesenchymal stromal cells. PLoS ONE 6, e20399 (2011).
- 77. Mindaye, S. T., Ra, M., Surdo, J. L., Bauer, S. R. & Alterman, M. A. Improved proteomic profiling of the cell surface of culture-expanded human bone marrow multipotent stromal cells. *J. Proteom.* 78, 1–14 (2013).
- 78. Lv, W. et al. The drug target genes show higher evolutionary conservation than non-target genes. Oncotarget 7, 4961–4971 (2015).
- 79. Minikel, E. V. et al. Evaluating drug targets through human loss-of-function genetic variation. Nature 581, 459-464 (2020).
- Bennett, C. N. & Green, J. E. Unlocking the power of cross-species genomic analyses: Identification of evolutionarily conserved breast cancer networks and validation of preclinical models. *Breast Cancer Res.* 10, 213 (2008).
- 81. Margiotta-Casaluci, L., Owen, S. F. & Winter, M. J. Cross-species extrapolation of biological data to guide the environmental safety assessment of pharmaceuticals—The State of the art and future priorities. *Environ. Toxicol. Chem.* https://doi.org/10.1002/etc.5634 (2023).
- Urbiola-Salvador, V., Miroszewska, D., Jabłońska, A., Qureshi, T. & Chen, Z. Proteomics approaches to characterize the immune responses in cancer. Biochim. Biophys. Acta Mol. Cell Res. 1869, 119266 (2022).
- 83. Deshpande, R., Sharma, S., Verfaillie, C. M., Hu, W.-S. & Myers, C. L. A scalable approach for discovering conserved active subnetworks across species. *PLoS Comput. Biol.* **6**, e1001028 (2010).
- 84. Ryaboshapkina, M. & Hammar, M. Tissue-specific genes as an underutilized resource in drug discovery. Sci. Rep. 9, 7233 (2019).
- 85. Joshi, T. & Xu, D. Quantitative assessment of relationship between sequence similarity and function similarity. *BMC Genom.* 8, 222 (2007).
- Godec, J. et al. Compendium of immune signatures identifies conserved and species-specific biology in response to inflammation. Immunity 44, 194–206 (2016).
- Shay, T. et al. Conservation and divergence in the transcriptional programs of the human and mouse immune systems. Proc. Natl. Acad. Sci. 110, 2946–2951 (2013).
- 88. Podder, A., Raju, A. & Schork, N. J. Cross-species and human inter-tissue network analysis of genes implicated in longevity and aging reveal strong support for nutrient sensing. *Front. Genet.* **12**, 719713 (2021).
- 89. Olivier, M., Berthon, P., Chastang, J., Cordier, G. & Lantier, F. Establishment and characterisation of ovine blood monocyte-derived cell lines. Vet. Immunol. Immunopathol. 82, 139–151 (2001).
- Keane, K. A., Mason, G. L. & DeMartini, J. C. Inhibition of nitric oxide enhances ovine lentivirus replication in monocyte-derived macrophages. Vet. Immunol. Immunopathol. 90, 179–189 (2002).
- 91. Arteche-Villasol, N. *et al.* Optimized in vitro isolation of different subpopulation of immune cells from peripheral blood and comparative techniques for generation of monocyte-derived macrophages in small ruminants. *Vet. Immunol. Immunopathol.* **230**, 110131 (2020).
- 92. Chan, S. S. M., Mcconnell, I. & Blacklaws, B. A. Generation and characterization of ovine dendritic cells derived from peripheral blood monocytes. *Immunology* **107**, 366–372 (2002).
- 93. Wattegedera, S. *et al.* Variability in cytokine production and cell proliferation by mitogen-activated ovine peripheral blood mononuclear cells: modulation by interleukin (IL)-10 and IL-12. *Vet. Immunol. Immunopathol.* **102**, 67–76 (2004).
- 94. Ciliberti, M. G. *et al.* Alterations in sheep peripheral blood mononuclear cell proliferation and cytokine release by polyunsaturated fatty acid supplementation in the diet under high ambient temperature. *J. Dairy Sci.* **98**, 872–879 (2015).

- 95. Rojas, C. A. A. *et al.* Time-course study of the transcriptome of peripheral blood mononuclear cells (PBMCs) from sheep infected with *Fasciola hepatica*. *PLoS ONE* **11**, e0159194 (2016).
- Khanduri, A. et al. Dysregulated miRNAome and proteome of PPRV infected goat PBMCs reveal a coordinated immune response. Front. Immunol. 9, 2631 (2018).
- Liu, Y. et al. Isolation and characterization of ovine monocyte-derived macrophages from peripheral blood. Vet. Immunol. Immunopathol. 205, 83–92 (2018).
- 98. Wang, S. et al. Transcriptional profiling of innate immune responses in sheep PBMCs induced by *Haemonchus contortus* soluble extracts. *Parasites Vectors* 12, 182 (2019).
- 99. Grieshaber-Bouyer, R. & Nigrovic, P. A. Neutrophil heterogeneity as therapeutic opportunity in immune-mediated disease. *Front. Immunol.* **10**, 346 (2019).
- 100. Jacobs, J. R., Middleton, D., Greiner, S. P. & Bowdridge, S. A. RNA-Sequencing of ovine PBMC after exposure to *Haemonchus contortus* larval antigen. *Parasite Immunol.* **42**, e12697 (2020).
- 101. Yang, J. et al. Baseline T-lymphocyte and cytokine indices in sheep peripheral blood. BMC Vet. Res. 18, 165 (2022).
- 102. Vallejo, R. et al. Effects of ovine monocyte-derived macrophage infection by recently isolated *Toxoplasma gondii* strains showing different phenotypic traits. *Animals* 12, 3453 (2022).
- 103. Windberger, U., Bartholovitsch, A., Plasenzotti, R., Korak, K. J. & Heinze, G. Whole blood viscosity, plasma viscosity and erythrocyte aggregation in nine mammalian species: Reference values and comparison of data. Exp. Physiol. 88, 431–440 (2003).
- 104. Varga, A. et al. Interspecies diversity of osmotic gradient deformability of red blood cells in human and seven vertebrate animal species. Cells 11, 1351 (2022).
- Corkum, C. P. et al. Immune cell subsets and their gene expression profiles from human PBMC isolated by vacutainer cell preparation tube (CPTTM) and standard density gradient. BMC Immunol. 16, 48 (2015).
- Betsou, F., Gaignaux, A., Ammerlaan, W., Norris, P. J. & Stone, M. Biospecimen science of blood for peripheral blood mononuclear cell (PBMC) functional applications. Curr. Pathobiol. Rep. 7, 17–27 (2019).
- 107. Bileck, A., Kreutz, D., Muqaku, B., Slany, A. & Gerner, C. Comprehensive assessment of proteins regulated by dexamethasone reveals novel effects in primary human peripheral blood mononuclear cells. *J. Proteome Res.* 13, 5989–6000 (2014).
- 108. Weiss, T. *et al.* Schwann cell plasticity regulates neuroblastic tumor cell differentiation via epidermal growth factor-like protein 8. *Nat. Commun.* **12**, 1624 (2021).
- 109. Humphrey, S. J., Karayel, O., James, D. E. & Mann, M. High-throughput and high-sensitivity phosphoproteomics with the EasyPhos platform. *Nat. Protoc.* **13**, 1897–1916 (2018).
- Cox, J. & Mann, M. MaxQuant enables high peptide identification rates, individualized p.p.b.-range mass accuracies and proteome-wide protein quantification. Nat. Biotechnol. 26, 1367–1372 (2008).
- 111. UniProt Consortium. UniProt: The universal protein knowledgebase in 2021. Nucleic Acids Res. 49, D480-D489 (2020).
- Szklarczyk, D. et al. STRING v11: Protein–protein association networks with increased coverage, supporting functional discovery in genome-wide experimental datasets. Nucleic Acids Res. 47, 1131 (2018).
- Szklarczyk, D. et al. The STRING database in 2021: Customizable protein-protein networks, and functional characterization of user-uploaded gene/measurement sets. Nucleic Acids Res. 49, 1074 (2020).
- 114. Szklarczyk, D. et al. The STRING database in 2023: Protein-protein association networks and functional enrichment analyses for any sequenced genome of interest. *Nucleic Acids Res.* 51, D638–D646 (2022).
- 115. Kanehisa, M., Furumichi, M., Sato, Y., Ishiguro-Watanabe, M. & Tanabe, M. KEGG: Integrating viruses and cellular organisms. Nucleic Acids Res. 49, 970 (2020).
- 116. The Gene Ontology Consortium. The Gene Ontology resource: Enriching a GOld mine. *Nucleic Acids Res.* **49**, D325–D334
- 117. Szklarczyk, D. et al. STRING v10: Protein-protein interaction networks, integrated over the tree of life. Nucleic Acids Res. 43, D447–D452 (2015).
- 118. Shannon, P. *et al.* Cytoscape: A software environment for integrated models of biomolecular interaction networks. *Genome Res.* 13, 2498–2504 (2003).
- Bandettini, W. P. et al. MultiContrast delayed enhancement (MCODE) improves detection of subendocardial myocardial infarction by late gadolinium enhancement cardiovascular magnetic resonance: A clinical validation study. J. Cardiovasc. Magn. Reson. 14, 83 (2012).
- 120. Chin, C.-H. et al. cytoHubba: Identifying hub objects and sub-networks from complex interactome. BMC Syst. Biol. 8, S11 (2014).
- 121. Zhao, Q., Zhang, Y., Shao, S., Sun, Y. & Lin, Z. Identification of hub genes and biological pathways in hepatocellular carcinoma by integrated bioinformatics analysis. *PeerJ* 9, e10594 (2021).
- 122. Xue, J. et al. The identification and validation of hub genes associated with acute myocardial infarction using weighted gene co-expression network analysis. J. Cardiovasc. Dev. Dis. 9, 30 (2022).
- 123. Hasan, Md. A. M., Maniruzzaman, Md. & Shin, J. Differentially expressed discriminative genes and significant meta-hub genes based key genes identification for hepatocellular carcinoma using statistical machine learning. *Sci. Rep.* 13, 3771 (2023).
- 124. Krämer, A., Green, J., Pollard, J. & Tugendreich, S. Causal analysis approaches in ingenuity pathway analysis. *Bioinformatics* 30, 523–530 (2014).
- 125. Shapiro, S. S., Wilk, M. B. & Chen, H. J. A comparative study of various tests for normality. *J. Am. Stat. Assoc.* 63, 1343–1372 (1968).
- 126. Fang, P. et al. Immune cell subset differentiation and tissue inflammation. J. Hematol. Oncol. 11, 97 (2018).
- Sivori, S. et al. Human NK cells: Surface receptors, inhibitory checkpoints, and translational applications. Cell. Mol. Immunol. 16, 430–441 (2019).
- 128. Wang, Y. *et al.* Immunophenotyping of peripheral blood mononuclear cells in septic shock patients with high-dimensional flow cytometry analysis reveals two subgroups with differential responses to immunostimulant drugs. *Front. Immunol.* **12**, 634127 (2021).
- 129. Tuomela, S. et al. Comparative analysis of human and mouse transcriptomes of Th17 cell priming. Oncotarget 7, 13416–13428 (2016).
- Tripathi, S. K. et al. Quantitative proteomics reveals the dynamic protein landscape during initiation of human Th17 cell polarization. iScience 11, 334–355 (2019).
- McClure, S. et al. Ontogeny, morphology and tissue distribution of a unique subset of CD4–CD8– sheep T lymphocytes. Immunol. Cell Biol. 67, 215–221 (1989).
- 132. Hayday, A. C. $\gamma\delta$ cells: A right time and a right place for a conserved third way of protection. *Immunology* **18**, 975–1026 (2000).
- 133. Holderness, J., Hedges, J. F., Ramstead, A. & Jutila, M. A. Comparative biology of γδ T cell function in humans, mice, and domestic animals. *Annu. Rev. Anim. Biosci.* 1, 99–124 (2013).
- 134. Hein, W. R., Dudler, L. & Morris, B. Differential peripheral expansion and in vivo antigen reactivity of α/β and γ/δ T cells emigrating from the early fetal lamb thymus. *Eur. J. Immunol.* **20**, 1805–1813 (1990).
- 135. Hein, W. R. & Mackay, C. R. Prominence of γδ T cells in the ruminant immune system. *Immunol. Today* 12, 30–34 (1991).
- Wilson, R. A., Zolnai, A., Rudas, P. & Frenyo, L. V. T-Cell subsets in blood and lymphoid tissues obtained from fetal calves, maturing calves, and adult bovine. Vet. Immunol. Immunopathol. 53, 49–60 (1996).

- 137. Lebedev, M., Faburay, B., Richt, J. A. & Young, A. Myeloid-like γδ T cell subset in the immune response to an experimental Rift Valley fever vaccine in sheep. *Vet. Immunol. Immunopathol.* **233**, 110184 (2021).
- 138. Mestas, J. & Hughes, C. C. W. Of mice and not men: Differences between mouse and human immunology. *J. Immunol.* 172, 2731–2738 (2004).
- 139. Gaudet, P., Livstone, M. S., Lewis, S. E. & Thomas, P. D. Phylogenetic-based propagation of functional annotations within the Gene Ontology consortium. *Brief. Bioinform.* 12, 449–462 (2011).
- 140. Haudek-Prinz, V. J. et al. Proteome signatures of inflammatory activated primary human peripheral blood mononuclear cells. J. Proteom. 76, 150–162 (2012).
- 141. Ciliberti, M. G. *et al.* Peripheral blood mononuclear cell proliferation and cytokine production in sheep as affected by cortisol level and duration of stress. *J. Dairy Sci.* **100**, 750–756 (2017).
- Lawlor, N. et al. Single cell analysis of blood mononuclear cells stimulated through either LPS or anti-CD3 and anti-CD28. Front. Immunol. 12, 636720 (2021).
- 143. Dinarello, C. A. Biologic basis for interleukin-1 in disease. Blood 87, 2095-2147 (1996).
- 144. Gaidt, M. M. et al. Human monocytes engage an alternative inflammasome pathway. Immunity 44, 833-846 (2016).
- 145. Nielsen, R. et al. A scan for positively selected genes in the genomes of humans and chimpanzees. PLoS Biol. 3, e170 (2005).
- 146. Fumagalli, M. et al. Signatures of environmental genetic adaptation pinpoint pathogens as the main selective pressure through human evolution. PLoS Genet. 7, e1002355 (2011).
- 147. Copeland, S. et al. Acute inflammatory response to endotoxin in mice and humans. Clin. Vaccine Immunol. 12, 60-67 (2005).
- 148. Carradice, D. & Lieschke, G. J. Zebrafish in hematology: Sushi or science? Blood 111, 3331-3342 (2008).
- 149. Cantrell, D. Signaling in lymphocyte activation. Cold Spring Harb. Perspect. Biol. 7, a018788 (2015).
- 150. Forn-Cuní, G., Varela, M., Pereiro, P., Novoa, B. & Figueras, A. Conserved gene regulation during acute inflammation between zebrafish and mammals. Sci. Rep. 7, 41905 (2017).
- 151. Menzies, M. & Ingham, A. Identification and expression of toll-like receptors 1–10 in selected bovine and ovine tissues. *Vet. Immunol. Immunopathol.* **109**, 23–30 (2006).
- 152. Hillman, N. H. et al. Toll-like receptors and agonist responses in the developing fetal sheep lung. Pediatr. Res. 63, 388–393 (2008).
- 153. Godsoe, A. et al. Cardiopulmonary changes with intermittent endotoxin administration in sheep. Circ. Shock 25, 61-74 (1988).
- 154. Murakami, K. et al. A novel animal model of sepsis after acute lung injury in sheep. Crit. Care Med. 30, 2083–2090 (2002).
- 155. Lange, M. et al. Continuously infused glipizide reverses the hyperdynamic circulation in ovine endotoxemia. Shock 27, 701–706 (2007).
- 156. Ertmer, C. et al. Methylprednisolone reverses vasopressin hyporesponsiveness in ovine endotoxemia. Shock 27, 281-288 (2007).
- 157. Enkhbaatar, P. et al. Novel ovine model of methicillin-resistant *Staphylococcus aureus*-induced pneumonia and sepsis. *Shock* 29, 642–649 (2008).
- 158. Lange, M. et al. Pulmonary microvascular hyperpermeability and expression of vascular endothelial growth factor in smoke inhalation- and pneumonia-induced acute lung injury. Burns 38, 1072–1078 (2012).
- Modi, W. S. & Yoshimura, T. Isolation of novel GRO genes and a phylogenetic analysis of the CXC chemokine subfamily in mammals. Mol. Biol. Evol. 16, 180–193 (1999).
- Du, Y. et al. Differential subnetwork of chemokines/cytokines in human, mouse, and rat brain cells after oxygen-glucose deprivation. I. Cereb. Blood Flow Metab. 37, 1425–1434 (2016).
- 161. Jarczak, J., Kaba, J., Reczyńska, D. & Bagnicka, E. Impaired expression of cytokines as a result of viral infections with an emphasis on small ruminant lentivirus infection in goats. *Viruses* 8, 186 (2016).
- 162. Mogensen, T. H. Pathogen recognition and inflammatory signaling in innate immune defenses. *Clin. Microbiol. Rev.* 22, 240–273
- Koppenol-Raab, M. et al. Proteome and secretome analysis reveals differential post-transcriptional regulation of toll-like receptor responses. Mol. Cell. Proteom. 16, S172–S186 (2017).
- Korbecki, J., Bobiński, R. & Dutka, M. Self-regulation of the inflammatory response by peroxisome proliferator-activated receptors. *Inflamm. Res.* 68, 443–458 (2019).
- 165. Meier-Soelch, J. et al. Monitoring the levels of cellular NF-κB activation states. Cancers 13, 5351 (2021).
- Eichelbaum, K. & Krijgsveld, J. Rapid temporal dynamics of transcription, protein synthesis, and secretion during macrophage activation. Mol. Cell. Proteom. 13, 792–810 (2014).
- 167. Rothenberg, D. A. *et al.* A proteomics approach to profiling the temporal translational response to stress and growth. *iScience* **9.** 367–381 (2018).
- 168. Lu, J. *et al.* Temporal proteomic profiling reveals functional pathways in vaccinia virus-induced cell migration. *Front. Microbiol.* **14**, 1185960 (2023).
- Chen, R. et al. In vitro response of human peripheral blood mononuclear cells (PBMC) to collagen films treated with cold plasma. Polymers 9, 254 (2017).
- 170. Pinna, S. *et al.* Proteomic analysis of human plasma and peripheral blood mononuclear cells in systemic lupus erythematosus patients. *J. Immunol. Methods* **446**, 37–46 (2017).
- 171. Silva, C., Santa, C., Anjo, S. I. & Manadas, B. A reference library of peripheral blood mononuclear cells for SWATH-MS analysis. *Proteom. Clin. Appl.* 10, 760–764 (2016).
- 172. Wu, T. *et al.* Comprehensive transcriptome profiling of peripheral blood mononuclear cells from patients with sepsis. *Int. J. Med. Sci.* 17, 2077–2086 (2020).
- 173. Jiang, N. et al. A data-independent acquisition (DIA)-based quantification workflow for proteome analysis of 5000 cells. J. Pharm. Biomed. Anal. 216, 114795 (2022).

Author contributions

A.E.: study design, data acquisition, analysis and interpretation, manuscript preparation; I.G and C.G.: study design, data acquisition and analysis; A.B. and G.O.: data acquisition; F. J.: study conception and design, data analysis and interpretation, manuscript preparation. All authors reviewed the manuscript.

Competing interests

The authors declare no competing interests.

Additional information

Supplementary Information The online version contains supplementary material available at https://doi.org/10.1038/s41598-024-66059-0.

Correspondence and requests for materials should be addressed to F.J.

Reprints and permissions information is available at www.nature.com/reprints.

Publisher's note Springer Nature remains neutral with regard to jurisdictional claims in published maps and institutional affiliations.

Open Access This article is licensed under a Creative Commons Attribution 4.0 International License, which permits use, sharing, adaptation, distribution and reproduction in any medium or format, as long as you give appropriate credit to the original author(s) and the source, provide a link to the Creative Commons licence, and indicate if changes were made. The images or other third party material in this article are included in the article's Creative Commons licence, unless indicated otherwise in a credit line to the material. If material is not included in the article's Creative Commons licence and your intended use is not permitted by statutory regulation or exceeds the permitted use, you will need to obtain permission directly from the copyright holder. To view a copy of this licence, visit http://creativecommons.org/licenses/by/4.0/.

© The Author(s) 2024